Nano Research 2018, 11(9): 4468–4488
https://doi.org/10.1007/s12274-018-2064-2
Review Article
ISSN 1998-0124
CN 11-5974/O4

Flexible surface-enhanced Raman scattering-active substrates based on nanofibrous membranes

Ekaterina S. Prikhozhdenko[1] (✉), Daniil N. Bratashov[1], Dmitry A. Gorin[1,2], and Alexey M. Yashchenok[1,2] (✉)

[1] *Remote Controlled Theranostic Systems Lab, Education and Research Institute of Nanostructures and Biosystems, Saratov State University, 83 Astrakhanskaya Str., Saratov 410012, Russia*
[2] *Skoltech Center for Photonics and Quantum Materials, Skolkovo Institute of Science and Technology, Skolkovo Innovation Center, 3 Nobel Str., Moscow 143026, Russia*

Received: 3 January 2018
Revised: 24 February 2018
Accepted: 23 March 2018

KEYWORDS
paper,
electrospun membrane,
fabric,
surface-enhanced Raman spectroscopy,
on-site diagnostics,
swabbing

ABSTRACT

Surface-enhanced Raman scattering (SERS) has emerged as an excellent analytical tool for the effective detection and fingerprint identification of various chemicals. Recently, significant progress has been made in the fabrication of SERS-active substrates using simple, inexpensive, and affordable methods. The full potential of universal SERS diagnostics will likely be realized with the development of approaches and devices capable of effectively detecting analytes on various surfaces as well as in multicomponent media. In addition, the combination of implantable or wearable SERS-active substrates and remote portable devices enables real-time diagnostics that ideally fit the concept of personalized medicine. In this paper, we summarize recent achievements in fabricating flexible SERS substrates made of cellulose paper, polymer membranes, and textile fibrous films. Emphasis is placed on the *in-situ* extraction and detection of various chemicals in real-world surfaces and complex media using flexible nanofibrous SERS platforms. The potential SERS applications and future perspectives in on-site diagnostics are also discussed.

1 Introduction

The first evidence of Raman signal enhancement obtained with pyridine molecules on the roughed silver surface by Fleischmann and coworkers has attracted tremendous interest from the vibrational spectroscopy community [1]. In particular, after the detailed studies of Raman amplification performed independently by Jearmaire and Van Duyne along with Albrecht and Creighton, it became clear that the signal enhancement is caused by the electromagnetic (EM) field rather than the saturation of molecules on the electrode surface [2, 3]. A few years later, Otto observed the charge transfer between molecules and a metal surface, which is now referred to as chemical enhancement [4]. Over the next few years, Creighton, Moskovits, and Suh independently formulated the surface selection rules [3, 5], while Kneipp and Hilderbrandt

Address correspondence to Ekaterina S. Prikhozhdenko, prikhozhdenkoes@gmail.com; Alexey M. Yashchenok, A.Yashchenok@skoltech.ru

performed the first assessment of the enhancement factor (EF) [6, 7]. Today this phenomenon is known as surface-enhanced Raman scattering (SERS). SERS can lead to an increase in the Raman cross-section by several orders of magnitude, up to approximately 10^{-16} cm^2/molecule [8], which is comparable with the fluorescence cross-section (10^{-15} cm^2/molecule). Unlike fluorescence, SERS can also increase the spatial resolution (potentially down to 10 nm), due to the strong localization of electromagnetic fields either at the interparticle junctions or on the small tips or edges of the SERS probes [9–11]. Renewed interest in SERS has been triggered by the development of single-molecule detection techniques [12, 13], which opened new avenues for the applications of this approach in biology [14–16], catalysis [17–20], bioimaging [21, 22], medicine [23–26], and other related fields.

In the last two decades, significant progress in the fabrication of SERS-active substrates has been achieved thanks to various advances in material science, surface chemistry, and nanotechnology. Top-down [27] and bottom-up [11, 28] approaches are the two main strategies applied to fabricate SERS substrates. Top-down approaches, such as nanosphere lithography [29, 30], nanoimprint lithography [31, 32], oblique angle metal film evaporation [33, 34], and e-beam deposition [35] were used to create uniform hotspot regions within various nanostructures [36, 37], which resulted in highly effective and reproducible SERS substrates [38, 39]. Bottom-up approaches, such as chemical synthesis [40], self-assembly [41–45], electrodeposition [46], dip-coating [47], and capillary force [48, 49] techniques were also successfully employed to fabricate SERS substrates.

In most cases, the application of SERS substrates requires a rational design and therefore appropriate manufacturing methods. For instance, colloidal nanoparticles aggregated in clusters or assembled on various surfaces are suitable for applications in aqueous and biological systems [50–58]. The combination of superhydrophobic surfaces and nanoparticles is effective for the localization and detection of the molecules of interest in a highly diluted sample [59]. A number of studies focused on hydrogel-like SERS substrates, which could generate hotspots upon collapse at high temperature and drying [60–69], and at the same time entrap molecules in a hydrogel matrix while in the swollen state. In addition, recyclable molecular trapping using hydrogel-based SERS sensors was also demonstrated [70]. Lee et al. achieved remote SERS sensing by the excitation of plasmons propagating back to the originally excited ends of periodically arranged silver nanowires (AgNWs) embedded in alumina [71]. To attain molecular bioimaging with high sensitivity as well as high spatial and temporal resolutions, high-throughput SERS nanotags with multiplexing capacity and comprising "bright" Raman reporters were developed [72–79]. A hollow-core photonic crystal fiber is another example of SERS platform for highly sensitive protein detection in a small volume [80, 81]. The combination of a fiber optic-based Raman spectroscopy device and tumor-targeting SERS nanoparticles could not only improve early cancer detection, but also accurately discriminate between malignant and normal tissues *in vivo* [82].

Despite the abundance of different SERS substrates with applications in various fields, novel design concepts, search for new materials, and integration with established analytical methods still are actively developing areas now. In this respect, the integration of organic matrix such as cellulose and polymeric meshes, hydrogels, foams, fabric with inorganic nanoparticles represents a very attractive approach for the fabrication of nanostructured systems with multiplexing functionalities. In this review, we summarize the latest achievements and ongoing studies in the fabrication and application of cellulose paper, polymeric electrospun nanofiber membranes, and textile materials in SERS diagnostics. Attention is devoted to methods used for the fabrication of nanofibrous flexible SERS substrates, the types of plasmonic nanoparticles impregnated in such types of SERS platforms, as well as the properties and SERS performance of nanofibrous substrates. In addition, we discuss the molecular detection capabilities of flexible nanofibrous SERS membranes over various surfaces, separation methods for multicomponent media based on chromatography- and ultrafiltration-based approaches, as well as recent advances in on-site SERS diagnostics.

2 SERS-active cellulose paper substrates

The intrinsic properties of paper, such as high surface-to-volume ratio, porosity, biocompatibility,

and biodegradability are very attractive for diagnostic applications. Paper is flexible and potentially compatible with printing technologies for designing low-cost microanalytical chips [83]. Moreover, paper can be used as a swab for collecting specimens on an uneven surface without active pumping [84]. In addition, cellulose fibers can be easily functionalized with polymers [85], metal nanoparticles [86–89], DNA/antibody-conjugated noble metal nanoparticles [90–92], dyes [93, 94], and carbon-based building blocks [95–97]. Chromatographic paper has been extensively used in analytical chemistry and diagnostics in the form of litmus paper, pregnancy strips, and urine test dipsticks.

In the recent years, substantial efforts have focused on impregnating paper substrates with metal nanoparticles (Table 1). Unlike paper treated with dyes, metal nanoparticles (and in particular noble metal ones) can improve the sensitivity, selectivity, and homogeneity of an output signal. Another unique feature of paper-based substrates is that they can be used as a stabilizing platform for plasmonic nanoparticles. The nanoparticles impregnated on paper are more stable in a variety of conditions compared to nanoparticles in solution, which is a very attractive feature in terms of controlled chemical modification and application of the nanoparticles, for instance in combinatorial chemistry [98]. Ross and

Table 1 Comparison of the performance of the most powerful paper-based SERS substrates

Fabrication method	Type of paper	Type of nanoparticles	EF	LOD[a]	RSD[b]	Ref.
Self-assembly	Whatman	AuNR AuBP	~ 5×10^6	1 nM (BPE[c] on AuNR) 0.5 nM (BPE[c] on AuBP)	~ 15%	[103]
		AgNP	2.2×10^7	1 nM (R6G) 50 nM (MG)	13.7% (inner ring) 14.4% (outer ring)	[107]
	Filter paper	AgNP	4×10^7	10 nM (4-MBA[d]) 50 nM (RB[e] in water) 1 μg/g (RB[e] in chili powder)	8.08% (spot-to-spot) 8.65% (batch-to-batch) < 5% (RB[e])	[78] [106]
	CPAM treated and untreated filter paper	AuNP	~ 2×10^8	1 nM (4-ATP)	~ 12% (treated) ~ 29% (untreated)	[105]
Pen-on-paper	A4 photocopy paper	AgNP AuNP AuNR	2×10^5 (λ = 532 nm) 1.5×10^5 (λ = 785 nm)	1 pM (R6G) 20 ppb (thiabendazole)	10%–20%	[101]
Electroless plating	Filter paper	AgNP	1.9×10^7 (p-NTP[f]) 1.4×10^7 (p-ATP) 7.8×10^8 (p-MBA[d])	625 nM (Tyrosine)	~ 4.5%	[108]
	Whatman	AuNP	7.9×10^8	1 pM (2-NAT[g])	~ 7.5%	[109]
Photo-induced	Copier paper; tissue paper; chromatography paper; filter paper	AgNP	2×10^6 (R6G) 1×10^5 (MG) 8×10^4 (p-ATP)	1 pM (R6G by swabbing) 104 ng/cm^2 (thiram by swabbing)	~ 10% (1 mM of R6G)	[110]
Screen printing	Filter paper	AgNP	4.4×10^6	0.16 pM (R6G) 10 nM (L-tryptophan) 0.7 μM (L-phenylalanine) 8.3 nM (adenosine) 0.78 nM (FMN[h])	< 10% (R6G)	[111]

[a]LOD: limit of detection; [b]RSD: relative standard deviation; [c]BPE: trans-1,2-bis(4-pyridyl)ethane; [d]MBA: mercaptobenzoic acid; [e]RB: Rhodamine B; [f]NTP: nitrothiophenol; [g]2-NAT: 2-naphthalenethiol; [h]FMN: flavin mononucleotide.

coworkers have used filter paper to study the EF variation as a function of the nanoparticle size [99]. The authors demonstrated that filter paper could be used to stabilize deliberately aggregated gold nanoparticles (AuNPs), maximizing the SERS enhancement. An intermediate degree of aggregation resulted in the largest enhancement observed for 20-nm AuNPs, whereas a further increase in the degree of aggregation was found to reduce the EF. A generalized Mie simulation showed that the highest measured EF likely originated from linear clusters, such as dimers, trimers, and tetramers.

2.1 Self-assembly methods

Tian and coworkers have developed a localized surface plasmon resonance (LSPR) sensor based on plasmonic paper decorated with biofunctionalized gold nanorods (AuNRs) [100]. Using the LSPR paper sensor, the authors could detect aquaporin-1, a biomarker for renal cancer carcinoma in artificial urine, in a label-free manner. Polavarapu et al. have presented a universal "pen-on-paper" approach for creating SERS substrates on common A4 photocopy paper [101]. The authors employed various plasmonic inks made of silver nanoparticles (AgNPs), AuNPs, and AuNRs to write SERS arrays tuned for different excitation wavelengths. The SERS-active spots on a paper written by the pen-on-paper method demonstrated strong sensitivity to Rhodamine 6G (R6G) and malachite green (MG) at concentrations down to 10 aM, as well as to the thiabendazole pesticide (20 ppb). The sensitivity of the paper detection technique was extended to the sub-nanogram range by premixing of the dyes and silver hydrosols before spotting the mixture on the filter paper [102]. The authors impregnated gold bipyramids (AuBPs) in filter paper and could detect 1,4-benzenedithiol (1,4-BDT) at concentrations down to 0.5 nM, with a low variation of SERS intensity (less than 15%) [103]. Ngo et al. studied the effect of AuNP concentration and three-dimensional (3D) particle distribution in filter paper on the SERS performance of the obtained substrates [104]. The AuNP content in the paper was increased from 1.8% to 22% with respect to the concentration of AuNPs, and only 40% of the AuNPs were located on the surface of the paper, while the rest was uniformly distributed in its volume. The EF of 4-aminothiophenol (4-ATP) linked to the AuNPs loaded onto the paper was estimated to be more than one order of magnitude higher than that of AuNPs on a silicon substrate. The authors then studied the role of a cationic polymer (polyacrylamide, CPAM) on the distribution of AuNPs in a SERS substrate and its influence on the EF. It was found that the high concentration, the high charge density, and high molecular weight of CPAM led to a uniform distribution of AuNP aggregates in paper, with minor desorption of AuNPs during SERS measurements [105]. Hasi and coworkers decorated filter paper with AgNPs at the interface of two immiscible liquids [106]. Using this approach, the surface coverage of AgNPs on paper was significantly improved, which led to a highly reproducible SERS signal (with a variation of less than 9%) and a long shelf life of the SERS substrates (about 1 month).

Filter paper strips decorated with AuNPs by multiple dipping into a concentrated AuNP solution were tested for monitoring the conversion of 4-nitrothiophenol (4-NTP) into 4-ATP [112]. The AuNP-loaded substrates showed very good SERS activity, with 10%–15% variation of the output signal at excitation wavelengths of 633, 785, and 830 nm. He and coworkers studied the impact of the concentration of gold nanostars (AuNSs) on their loading onto paper substrates [113]. Multiple drips of filter paper into an AuNS solution were found to produce a higher enhancement factor, compared to A4 printing paper and two commercial Au/Ag SERS substrates. The important finding of this study was that the SERS signal could be measured immediately after dripping of the analytes in a liquid. Mehn et al. successfully fabricated paper-based SERS substrates consisting of spherical and star-like AuNPs on standard filter paper supports [114]. They found that the presence of citrate during the deposition of AuNPs improves the surface density and homogeneity of AuNPs in the paper supports. The presence of high citrate concentrations (100 mM) upon deposition of AuNPs results in excellent SERS performance. The paper-based SERS substrates were found to be suitable for the detection of MG and for monitoring the oxidation products of the drug apomorphine, used for the management of Parkinson's disease.

2.2 Printing methods

White's group established inkjet printing as an effective tool for fabricating highly sensitive paper-based SERS substrates [115]. The 1-mm SERS active spots of AgNPs impregnated in hydrophobic paper showed excellent sensitivity to R6G, at concentrations down to 10 fM. Nitrocellulose and cellulose papers inkjet-printed with AuNPs were successfully tested for the detection of BPE at concentrations as low as 1.8 ppb using a portable Raman spectrometer. In addition, the same substrates were used to detect two fungicides, MG (1 ppb) and thiram (10 ng), in water and on a glass substrate [116]. SERS active pads were fabricated via *in situ* growth of AuNPs on untreated A4 paper using an inkjet printer [117]. A bio-ink consisting of a mixture of lecithin and potassium iodide was first printed on paper, and the obtained samples were then immersed in an aqueous solution of $HAuCl_4$ for synthesizing gold nanoparticles. The SERS strips were tested for the detection of biotoxins in food and exhibited maximum residue levels of MG and iprodione of 10 μM and 1 nM, respectively. A simple method for fabricating disposable and highly reproducible SERS arrays on woven films using screen-printing was also demonstrated [111]. Using this technique, the authors printed silver arrays on woven substrates in a large batch (6 × 10 printed spots). The impact of the fabrication conditions on the SERS detection of R6G and biological molecules was studied. A low variation (< 10%) of the SERS intensity of the main R6G peaks and a good long-term stability (about 12 weeks) of the SERS substrates were observed. The authors studied different types of paper substrates impregnated with AgNWs and measured the SERS signal intensity relative to a fluorescent background [110]. SERS substrates made of tissue paper maintained a similar SERS activity under light irradiation for 12 months after their preparation, while a 4-fold reduction of the SERS activity was observed after 16 months at ambient conditions.

2.3 Physical vapor deposition

Zhang et al. fabricated SERS paper strips by coating printing, filter, napkin, and sulfate paper as well as newspaper with silver nanolayers via physical vapor deposition [118]. All types of SERS strips enabled the highly sensitive SERS detection of R6G, in concentrations as low as 1 nM. The resulting SERS stripes remained active for 13.5 h, and the storage period could be further extended under a nitrogen atmosphere. Fan and coworkers developed an interesting SERS platform made of sandpaper coated with a 200-nm silver film obtained by vacuum deposition [119]. The authors showed that these substrates were not only capable to detect Nile Blue A (NBA) down to pM concentrations, but could also be used as swabs to probe the pesticide triazophos on real-world surfaces. Silver nanorod arrays formed on a filter membrane via oblique angle deposition were used for the rapid concentration and detection of bacteria by the SERS method [120]. Using these types of SERS substrates, the limit of detection (LOD) of *E. coli* in a sample volume of 10 mL was decreased by approximately two times.

2.4 Electroless plating

Filter paper with a high density and uniform distribution of AgNPs on the paper fibers was manufactured using the electroless plating procedure [121]. To evaluate the SERS performance of the AgNP-decorated paper, two different approaches were used. In the first one (dynamic SERS, D-SERS) the SERS signal was acquired during the evaporation of a solvent, whereas in the other approach the SERS spectra were collected after full evaporation of the solvent. The D-SERS method demonstrated better SERS detection of crystal violet (CV) at concentrations from 10^{-7} to 10^{-9} M and improved reproducibility, with relative standard deviation (RSD) of less than 20%. A two-fold decrease in the SERS signals was found after long-term storage. Cheng and coworkers systematically studied the impact of the pretreatment procedure on the surface properties and SERS signals of filter paper covered by electroless plating [108]. The filter paper treated with ammonia exhibited the lowest variation of SERS signals (less than 8%) and the highest EF (~ 10^7) among all pretreatment reagents. The filter-based SERS substrates demonstrated a higher selectivity to tyrosine comparing to other amino acids in aqueous solution. The detection limit was found to be about 625 nM after 10-min immersion of the substrates in a test solution. Kim and coworkers fabricated gold-coated

hydrophilic spots on wax-printed porous paper strips through the successive ionic layer absorption and reaction (SILAR) method [109]. The concentration of the reactive solution and the number of SILAR cycles were optimized to achieve maximum SERS activity. The gold-coated paper strips exhibited an enhancement factor of 7.8×10^8, as well as high reproducibility (RSD ~ 7.5%) and sensitivity to 2-naphthalenethiol (2-NAT, 1 pM). A label-free biofluid sensing approach for the early detection of eye infection diseases has also been demonstrated.

2.5 Photoinduction approaches

Yu et al. developed a SERS substrate by decorating paper with both AgNPs and AuNPs through a single-shot laser-induced photothermal effect [122]. The influence of the material properties and of a different number of laser pulses on the formation of the nanoparticles was studied. The surface morphology and thermal conductivity of the substrates turned out to be the two main factors influencing the growth of nanoparticles. The authors also found that three types of paper with different pore sizes resulted in different nanoparticle densities on the paper filters. Detection limits of 10^{-15} M for R6G and 10^{-18} M for 4-ATP were found using filter paper with a pore size of 2.5 μm.

3 Electrospun nanofiber membranes as SERS substrates

Polymer nanofiber mesh fabricated by electrospinning is another example of nanofibrous 3D membrane suitable for the synthesis of highly sensitive SERS substrates. Similar to paper, the electrospun nanofiber films are flexible and have a porous structure as well as a high specific surface area. Moreover, their pore sizes can be controlled by varying the process conditions, whereas the surface functional groups are dependent on the types of polymers used in the fabrication of the polymeric mesh [123–125]. In addition, most electrospun nanofiber films are intrinsically hydrophobic, which makes them excellent materials for the concentration of analyte molecules without specific treatments to prevent their random spreading, unlike wax-printed paper.

A number of methods were developed for incorporating metal nanoparticles into electrospun polymer films [126]. For the sake of simplicity, they can be divided into three main classes: i) dispersion of either metal salts or preformed metal nanoparticles into a polymer solution, followed by spinning of the mixture to obtain functionalized nanofibrous membranes; ii) surface and bulk modification of preformed polymer nanofiber substrates; iii) *in situ* synthesis of plasmonic nanoparticles through chemical, thermal, or laser reduction of metal precursors dispersed in the polymer matrix. All these methods have been used to fabricate SERS-active electrospun nanofiber membranes of adequate quality in terms of nanoparticle distribution in the polymer matrix, Raman signal enhancement, and SERS performance (Table 2).

3.1 Electrospinning of premixed polymer solution

He et al. reported the first fabrication of SERS substrates based on composite biocompatible polyvinyl alcohol (PVA) nanofibers [127]. The authors incorporated AgNPs in the PVA matrix by premixing the AgNPs and a PVA solution, followed by electrospinning. The resulting AgNP/PVA nanofiber films (80 cm^2) composed of frozen silver dimers and chain-like aggregates were protected from the environment by the polymer matrix. It was found that dimers and short chain-like aggregates in the PVA matrix provided the highest Raman signal enhancement observed among the substrates fabricated in the experiment. The obtained AgNP/PVA films showed a low variation of SERS signal (less than 7%) even after one year of storage in air. Zhang and coworkers presented a facile self-assembly method to control the alignment of AuNRs in an electrospun PVA nanofiber mat [128]. Using this approach, free-standing, flexible, and stable AuNR/PVA nanofibrous membranes with broad absorption bands were obtained. The resulting mats were found to be effective for the SERS detection of 3,3′-diethylthiatricarbocyanine iodide (DTTCI) at trace levels of 10^{-7} M, with a SERS intensity RSD of 10%.

3.2 Surface and bulk modifications

Bao et al. have developed SERS-active polymethacrylic acid (PMAA) nanofibrous membranes by seed-mediated electroless plating growth of AgNPs [129]. To activate

Table 2 SERS performance of the most efficient electrospun nanofiber membranes and textiles

Fabrication method	Type of paper	Type of nanoparticles	EF	LOD	RSD	Ref.
Drop-casting	P2VP[a]	AuNR	1.2×10^5	10 nM (4-ATP) 0.1 μM (R6G)	< 10%	[131]
Electrodeposition	PA[b]	AgNSh[h]	1.1×10^7	1 μM (PCB-3[i])	< 15%	[132]
Electrospinning	PVA	Ag-dimers	1.0×10^9	1 μM (4-MBA)	< 7%	[127]
In situ synthesis	Chitosan	AuNP	2.9×10^5	1 fM (2-NAT) 10 μM (R6G) 1 μg/mL (glucose)	~ 28%	[133]
Photo-induced	PMAA/PVP[c]	AgNP	3.1×10^5	0.1 μM (MG)	0.2%	[134]
	Agar/PAN[d]	AgNP	4.8×10^5	10 ppb (R6G)	< 22%	[135]
Physical vapor deposition	PVDF[e] PLLA[f] Nylon	Au-films	3.6×10^6	0.1 μM (p-MBA)	15%–17%	[136]
Self-assembly	Cotton swab	AgNP	1.6×10^6	0.78 fg (NBA on glass) ~ 1.2 ng/cm^2 (2,4-DNT[j] on glass)	36%–52% (spot-to-spot) ~ 20% (batch-to-batch)	[137]
Soaking	Cotton swab	AgNP	6.6×10^6	0.8 pM (R6G) 0.5 μM (carbaryl on a cucumber)	5%–10%	[138]
	PAA[g]/PVA	AuNP	2.2×10^7	10 pM (R6G)	2%–18%	[139]

[a]P2VP: poly(2-vinylpyridine); [b]PA: polyamide; [c]PVP: poly(N-vinylpyrrolidone); [d]PAN: polyacrylonitrile; [e]PVDF: poly(vinylidene fluoride); [f]PLLA: poly(L-lactide acid); [g]PAA: poly(acrylic acid); [h]AgNSh: silver nanosheets; [i]PCB-3: polychlorinated biphenyl-3; [j]2,4-DNT: 2,4-dinitrotoluene .

the hydrophilic groups and facilitate the linkage of platinum seeds, the surface of PMAA nanofibers was treated with oxygen plasma. Zhang et al. developed SERS substrates made of polyacrylonitrile (PAN) nanofibers surface-functionalized with AgNPs and amidoxime via a seed-mediated growth process [130]. The reaction time and stirring rate were used to control the density and size of AgNPs in the polymer matrix.

These substrates demonstrated excellent sensitivity to R6G concentrations as low as 10 ppb. Moreover, the AgNP/PAN membranes showed very good mechanical flexibility/resilience properties. Lee and coworkers demonstrated a nearly uniform distribution of AuNRs on the surface of electrospun poly(2-vinylpyridine) (P2VP) nanofibers obtained using a drop-cast technique [131]. It was found that gaps between well-oriented nanofibers were responsible for the alignment of AuNRs along the nanofibers. A comparative study showed a 50-fold SERS enhancement for well-aligned Au nanorods and oriented nanofibers relative to planar substrates. Moreover, the SERS intensity was strongly dependent on the orientation of the aligned AuNR nanofiber substrates with respect to the polarization of the incident light. Liu and coworkers studied poly(acrylic acid) (PAA)/PVA electrospun nanofibers decorated with positively charged AuNPs [139]. A thermal treatment of the PAA/PVA nanofibers transformed the surface from hydrophobic to hydrophilic and therefore facilitated further self-assembly of the AuNPs. These composite substrates demonstrated high SERS sensitivity, with trace levels of 10^{-8} and 10^{-7} M for 4-ATP and R6G, respectively. The relative standard deviations of the SERS intensity of the main peaks centered at 1,079 and 1,589 cm^{-1} were calculated to be 5.8% and 5.6%, respectively. Zhang et al. introduced a new approach based on the electrostatic attraction between AuNRs and AgNWs further embedded within PVA nanofibers [140]. AuNRs were arranged along AgNWs, while AuNR/AgNW building

blocks were assembled along the PVA nanofibers. The AuNR/AgNW PVA nanofibers showed highly sensitive SERS detection of DTTCI at concentrations down to 10^{-7} M, with a low SERS intensity deviation (~ 10%). It was suggested that the most intense EM fields were localized in the interstitial regions of AuNRs and at Au–Ag contact points. A layer-by-layer self-assembly method has been used to decorate the surface of electrospun nanofibrous 3D films of polycaprolactone (PCL) with AuNRs. A minimum of five polyelectrolyte layers was required to maximize binding and therefore achieve high packaging of AuNRs on the polyelectrolyte-modified surface of the PCL nanofibers. Due to the enhanced surface area of the 3D film, the AuNR/PCL mesh provided a six-fold increase in SERS intensity compared to its two-dimenional (2D) AuNR/PCL film counterpart. This fabrication protocol can be readily extended to the production of nanocomposite materials with various compositions and morphologies [141]. An enhancement in Raman and SERS signals was found for PMAA nanofiber films decorated with AuNRs [142]. The authors found that the nanofibrous substrates could lead to a 15-fold enhancement in the Raman signal compared to spin-cast films, thanks to the 3D structure of the PMAA films and the multiple scattering of incident irradiation by the nanofibers. A 10-fold amplification of the SERS signal after deposition of AuNRs on top of PMAA nanofibrous films was observed. Free-standing silver nanosheet (AgNSh)-grafted electrospun polyamide (PA) nanofibers were obtained by an electrodeposition approach [132]. The high density of "hotspots" within the interparticle junctions of the AgNShs and the large surface area of the 3D polymer network allowed the effective detection of R6G and environmental hazardous polychlorinated biphenyls. 3D composite AgNSh/PA nanofibers modified with mono-6-thio-β-cyclodextrin enabled detection of polychlorinated biphenyl-3 (PCB-3) at trace levels of 10^{-6} M. Wang et al. prepared SERS-active substrates on hydrophobic PCL nanofiber films, which were first exposed to UV light for 30 min and then incubated in a AuNP colloidal solution. The analytical capability of the films was demonstrated by using them for the detection of 4-ATP and 2-thiouracil (a thyroid inhibitor). The impact of the number of electrospun polymeric fiber layers of PCL on the SERS activity of the substrates was also investigated [143].

Zhang and coworkers applied the physical vapor deposition method to coat the surface of electrospun SU-8 (an epoxy-based photoresist) nanofiber films with a silver nanolayer [144]. The metal-coated SU-8 nanofibers deposited on a solid substrate were then patterned into grating microstructures by photolithography. These substrates exhibited excellent SERS activity for probing R6G molecules with trace levels of 10^{-8} M and a low variation in SERS intensity. Szymborski et al. applied physical vapor deposition for sputtering a 90-nm gold layer on electrospun poly(L-lactide acid) (PLLA), PVDF, and nylon nanofiber films [136]. The gold-coated films were proved effective for the SERS detection of both biological and non-biological samples. The important aspect of this study is that it established a novel approach for the immobilization of bacteria from various liquids by vacuum pumping of the samples. The study highlighted the potential of nanofibrous films based on metal-modified polymers for the fast detection of microorganisms in real-world applications.

3.3 *In situ* synthesis

AgNP/PMAA/poly(N-vinylpyrrolidone) (PVP) nanofibrous films were fabricated via *in situ* photoreduction of silver ions. It was found that the introduction of PMAA in the electrospun solutions significantly increased the absorbed amounts of silver ions in the nanofibers owing to its linear structure with a high content of carboxyl groups. A desk lamp and two ultraviolet (UV) lamps (254 and 365 nm) were employed to control the content and size of AgNPs in the polymer matrix. The samples obtained using the desk and 365 nm UV lamps as light sources showed very high SERS activity and small variation in the intensity of the main SERS peaks (0.2%). The practical application to the detection of MG in water, with recoveries between 94% and 102.5%, was also demonstrated [134]. Electrospun nanofibrous films of AgNP/agar/PAN composites were successfully fabricated by *in situ* photoreduction. The introduction of agar in the PAN matrix resulted in a high yield of stable AgNPs with uniform dispersion in the nanofibers. The AgNP/agar/PAN nanofiber films obtained by illumination with a 365 nm UV lamp demonstrated the highest SERS activity and reproducibility, with a RSD of less than 22%. These substrates were applied for the quantitative detection

of MG at concentrations as low as 0.1 M. The determination of MG in fishery, lake, and river water samples, with recoveries between 92.0% and 105.4%, was also demonstrated [135]. Ren et al. combined cellulose nanocrystals, silicon nanoparticles, PAN, and AgNPs to fabricate SERS-active nanofiber membranes with enhanced thermal stability [145]. In the study of Severyukhina et al., AuNPs were impregnated in chitosan electrospun nanofiber films by *in situ* synthesis using the modified Turkevich's method [133]. The SERS performance was studied by varying the concentration of AuNPs, and an average EF of 2×10^5 was obtained. Potential detection of D-glucose (an important biomarker of diabetes) was demonstrated, with a reliable SERS signal in the range from 1 μg/mL to 1 mg/mL.

4 Textile materials as SERS substrates

In the last few years, various studies have focused on natural materials for the fabrication of functional systems [146]. Textile fabric is a very attractive natural material, with a large number of chemical groups on the fiber surface; moreover, this material is flexible, soft, strong, lightweight and bio-friendly. Various textile products, such as wool [147, 148], cotton [149], and silk [141] have been impregnated with noble metal nanoparticles to impart antibacterial [149–151], self-cleaning, and UV protection properties [152, 153], as well as to enhance their thermal conductivity [154].

Following this trend, textile products impregnated with plasmonic nanoparticles are highly attractive for the development of wearable sensors capable of detecting and monitoring the concentration of chemicals on the skin or in the bodily fluids of the wearer or the levels of toxic agents in the environment surrounding the wearer. Recently, several groups have employed cloth and cotton products to fabricate SERS substrates with potential on-site applications as chemical sensors. Robinson et al. have demonstrated the use of metal-coated *zari* fabric (or "fab-chips") as an inexpensive SERS substrate for the first time [155]. The authors optimized three methods for the fabrication of fab-chips using AgNPs. They found that direct deposition of AgNPs on the *zari* substrates provided high sensitivity and uniformity of the SERS signal by probing 4,4'-bipyridine. Subsequently, they demonstrated the detection of adenine at concentrations as low as 0.01 mM. The latter results show the potential of fabric-based substrates to broaden the applications of SERS to wearable low-cost sensors. The *in situ* synthesis of AuNPs on a commercially available silk fabric using various concentrations of chloroauric acid as a gold precursor was also demonstrated [156]. The authors determined the optimal concentrations of the gold precursor for achieving the highest enhancement of the Raman signal of several analytes, such as 4-mercaptopyridine, *p*-aminothiophenol (p-ATP), and CV. The minimum detectable levels of the probed analytes were measured to be 10^{-9} M.

5 Methods for immobilization, extraction, and detection of analyte molecules

5.1 Swabs and dipsticks

The combination of paper dipsticks and the SERS method offers a viable opportunity for the ultrasensitive detection of analyte molecules. Tran et al. have combined a chronographic paper with a silver hydrosol for the first time [157]. A silver-coated filter was also used to separate binary mixtures for spatially resolved SERS with a short integration time [158]. Lee and coworkers have used commercially available laboratory filter papers to fabricate SERS substrates that demonstrated excellent sensitivity to 1,4-BDT residues (< 140 pg) by swabbing the samples across a glass surface [159]. A novel approach based on biomimetic recognition of target chemicals was developed by Nergiz et al. [160]. In this study, the authors used filter paper decorated with AuNRs and conjugated with phage-displayed trinitrotoluene-binding peptides. The peptide-coated plasmonic nanostructures enabled selective targeting of trinitrotoluene (down to 100 pM) both in water (dipstick configuration) and on an uncleaned glass surface (swabbing experiments), as well as in a complex organic medium such as shampoo.

In order to enhance the storage capacity of SERS-active nanostructures and, in particular, to prevent tarnishing of prefabricated silver SERS substrates, Joshi and Santhanam developed a print-expose-develop process [110]. This approach involves printing silver nitrate

and potassium halide solutions on paper using a desktop inkjet printer. The authors showed that the photo-induced silver halide transformed to a "latent" film with a large number of densely packed tubular grains, which remained stable for an unlimited period under atmospheric conditions. SERS-active silver paper was fabricated by immersing the substrates in a standard photographic developer solution, which resulted in the development of interconnected silver nanowires. Interestingly, the SERS activity of samples aged for 12 months under ambient conditions was not affected and remained identical to that of the as-prepared samples. The obtained SERS papers exhibited a low variation of the SERS signal, with a RSD of about 10%. The authors then applied the samples to detect R6G in concentrations as low as 1 pM by swabbing glass substrates with SERS papers. In addition, thiram surface concentrations down to 104 ng/cm^2 could be detected by swabbing apple peels with the same SERS substrates (Fig. 1). Microfluidic paper chips composed of a sample volume, detection reservoirs, and a channel were obtained using the wax-printing method [107].

Subsequently, the detection reservoirs were painted with a common painting brush to deposit AgNPs. By this approach, the optimal number of depositing cycles was found to be 14. The microfluidic paper SERS chips were then tested for the detection of R6G and MG. The RSD of the signal of the chips varied from 13.7% to 14.4% for inner and outer rings, respectively.

Reliable detection of R6G and MG was observed for concentrations from 5.0 × 10^{-6} to 1.0 × 10^{-9} M and from 1,000 to 50 nM, respectively. Multi-branched gold nanoparticles (MAuNPs) have been used to decorate filter paper for the SERS-mediated detection of chemicals and biomolecules, as well as of pesticides on a fruit peel. MAuNP-paper SERS platforms exhibited the highest enhancement factor (4.7 × 10^9) for SERS paper substrates. MAuNP-paper SERS dipsticks showed very low limit of detections for 1,4-BDT (100 pM) and human serum albumin (100 fM). Detection of 4-ATP at a concentration of 62.5 pg by swabbing MAuNP-paper substrates across a glass surface was demonstrated. A toxic organophosphate pesticide, methyl parathion, was probed by swabbing an apple with an MAuNP-paper substrate, which highlighted the potential real-world applications of these SERS substrates [161]. The Diagnostic anSERS, Inc. company demonstrated the transition of paper-based

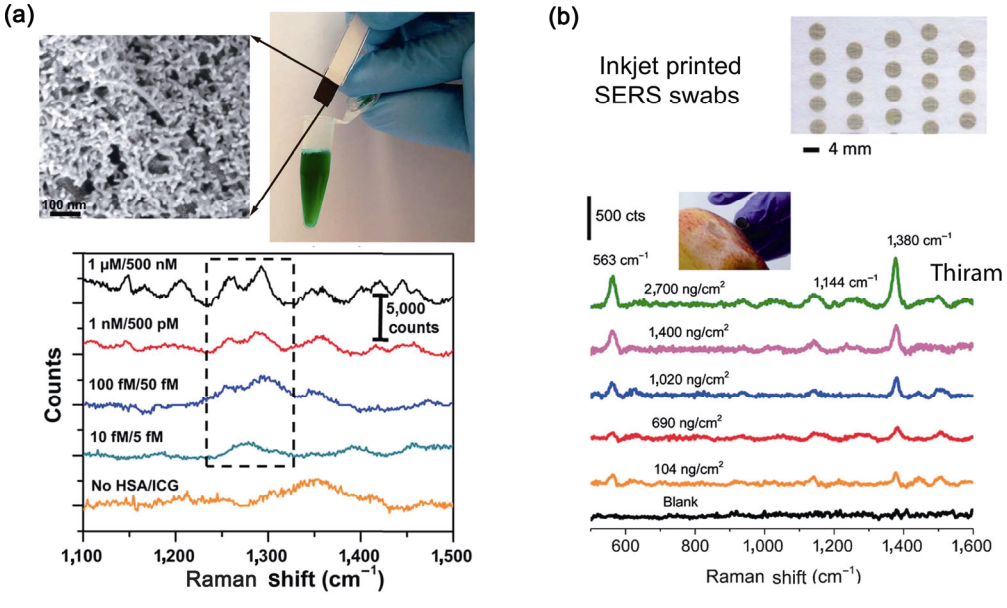

Figure 1 (a) SEM image of the different orientation of MAuNPs on a paper dipstick used for protein detection (top), and SERS spectra of different ratios of human serum albumin-indocyanine green mixture probed using a MAuNP-paper dipstick (bottom). (b) Photograph of inkjet-printed SERS-active substrates in swab form and corresponding SERS spectra of thiram swabbed from apple peels. (a) reprinted with permission from Ref. [161], © The Royal Society of Chemistry 2014; (b) reprinted with permission from Ref. [110], © The Royal Society of Chemistry 2016.

SERS substrates from the lab to market through a combination of functionalized P-SERS™ substrates with reader hardware from Innovative Photonic Solutions. P-SERS™ substrates were used for detecting drugs in saliva of vehicle drivers and could enable future cancer screening to be performed in the clinic [162].

Qu and coworkers developed a facile approach for the fabrication of highly sensitive, reproducible, and low-cost SERS substrates consisting of cotton swabs and AgNPs [138]. Cotton swabs loaded with AgNPs were used to detect R6G at concentrations down to 0.81 pM, with a low variation (5%–10%) in the SERS intensity of the main peaks. The use of SERS cotton swabs for the *in situ* probing of carbaryl on the rough surface of a cucumber has also been demonstrated. These flexible and highly robust SERS cotton swabs can be conveniently used for the stand-off SERS detection of dangerous residues. Cotton swabs were successfully transformed into SERS substrates (Q-tips) using either self-assembly of AgNPs or *in situ* growth of AgNPs on the surface of the cotton swabs [137]. The SERS Q-tips enabled reliable detection of both NBA and 2,4-dinitrotoluene (2,4-DNT) spilled on glass in small concentrations. The LOD was found to be two orders of magnitude lower than that obtained by fiber optic coupled absorption/reflection infrared spectroscopy or ion mobility spectrometry equipped with a mass spectrometer. Furthermore, the 2,4-DNT powder could be identified by direct swabbing on glass, even after the 27th touch with the 2,4-DNT contaminated finger. The SERS Q-tip substrates were found to be stable for approximately 1 month in ambient air.

5.2 Charge-selective separation

Plasmonic calligraphy has emerged as a facile and an effective approach to miniaturize the test domain size in LSPR detection, as well as to isolate the domains on a single test strip, which significantly improves the sensitivity of a plasmonic biosensor and facilitates multiplexed bio-detection [163]. The plasmon calligraphy approach was introduced as a simple and effective tool for charge-selective SERS detection of chemical analytes. Polyelectrolyte-coated AuNRs serve as isolated SERS domains for separating charged chemicals from a mixture of several compounds. The calligraphed substrates showed high sensitivity to analytes, together with excellent selectivity and low variation of SERS signal [164].

5.3 Lateral- and vertical-flow approaches

Inkjet-printed AgNP paper was used in swab and lateral-flow dipstick forms to detect R6G, malathion, and two illegal narcotics, heroin and cocaine, in concentrations as low as 95 fg, 413 pg, 15 ng, and 9 ng, respectively (Fig. 2) [165]. The capabilities of inkjet-printed SERS paper for the chromatographic separation of target analytes from complex samples have been further extended in Ref. [166]. The authors achieved one-dimensional (1D) and 2D separation of R6G, MG, and methylene blue using lateral-flow transport of analytes. In addition, a PVDF SERS membrane was used to separate and identify melamine in infant formula at concentrations as low as 5 ppm. The detection and quantification of trace quantities of heroin in a sample contaminated with IR780 infrared dye was also demonstrated. A vertical-flow membrane system with inkjet-printed SERS paper and a portable spectrometer were used to achieve low-cost monitoring of flucytosine in undiluted human serum [167]. The membrane system consisted of bare nitrocellulose filters stacked on the top of inkjet-printed SERS paper. To perform the vertical-flow separation, a sample droplet was loaded on top of the uppermost filters positioned directly at the nanoparticle region of the SERS sensor. Upon permeation through the filters, the serum components were stacked within the polymer mesh, while the remaining sample volume reached the underlying silver paper for further SERS identification. The vertical flow system was optimized in terms of membrane type, number of membranes, sample volume, assay time, serum dilution, and size of the microporous membranes. Nitrocellulose and PVDF used as filtering membranes allowed to effectively entrap the serum components while ensuring the vertical flow of flucytosine to the SERS sensor. After optimization, the system based on nitrocellulose and inkjet-printed SERS paper was used to achieve rapid quantitative detection of 10 μg/mL flucytosine in 100% serum (Fig. 2) [168]. These results pave the way for the separation of target analytes from complex biological

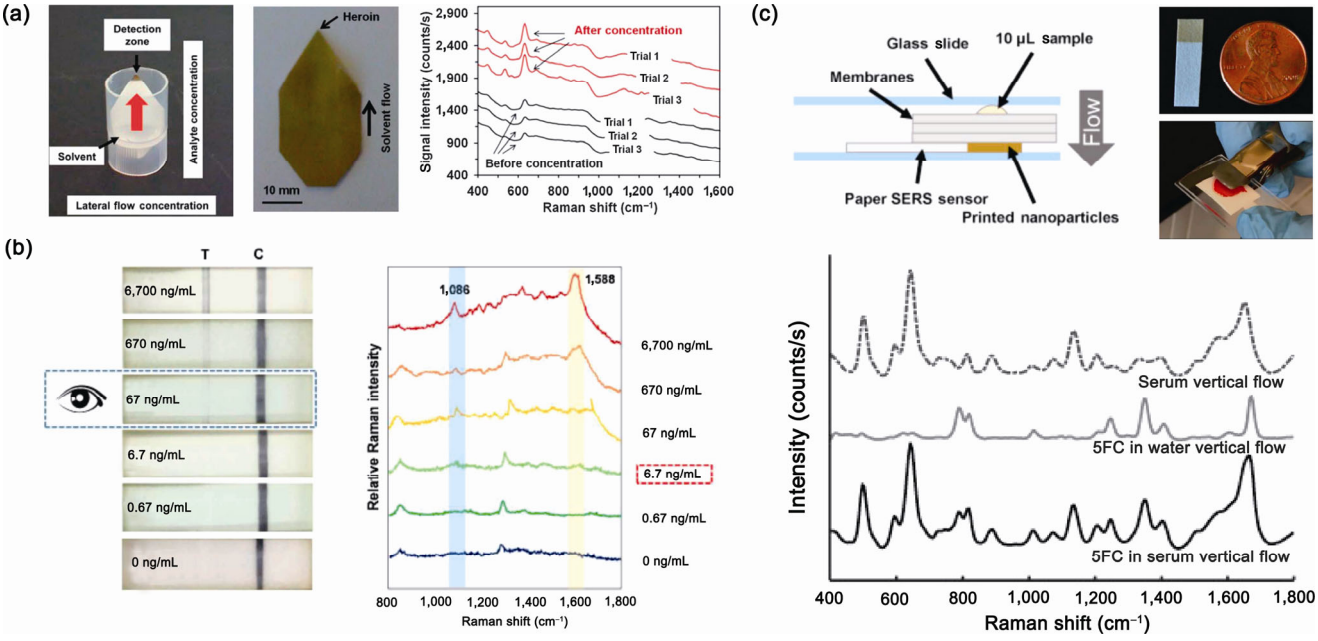

Figure 2 (a) Lateral-flow concentration of chemicals using paper; example of paper substrate with heroin localized on the tip after solvent flow and respective average SERS spectra of three separate measurement series before and after lateral concentration. (b) SERS-LFIA test strips impregnated with various concentrations of AuNS-ATP conjugated with monoclonal antibody for the qualitative visual detection of influenza A nucleoprotein (left) and quantitative analysis by SERS method (right). (c) Schematic illustration of device for vertical flow separation of chemicals from a multicomponent medium (top left), photographs of inkjet-printed SERS paper substrate and SERS sensor along with vertical flow setup (top right), and SERS spectra of 5-fluorocytosine (5FC) in water and serum after vertical flow. (a) reprinted with permission from Ref. [166], © The Royal Society of Chemistry 2013; (b) reproduced with permission from Ref. [169], © The Royal Society of Chemistry 2016; (c) reprinted with permission from Ref. [168], © SPIE 2017.

samples, exploiting the capabilities of SERS identification across the relevant therapeutic range. A SERS platform made of lateral-flow immunochromatographic assay (LFIA) test strips comprising antibody-conjugated AuNSs for the analysis of influenza A nucleoprotein was fabricated [169]. The combination of SERS and LFIA methods resulted in much higher detection sensitivity, compared with conventional methods (Fig. 2). The antibody-conjugated AuNSs in the SERS-LFIA system are highly specific to the influenza A virus, without interferences from other proteins and viruses. The system can be used to detect the influenza A antigen in complex biological matrices, such as infected allantoic fluid containing the influenza A (H1N1) pdm09 virus at 5.6×10^3 $TCID_{50}$/mL (50% tissue culture infectious dose). The real-world application of AgNP-decorated paper was demonstrated by using it to probe thiram in three kinds of fruits, with detection limits of 7.2 ng/cm^2 for bananas, 24 ng/cm^2 for apples, and 36 ng/cm^2 for tomatoes, respectively [121].

Remarkable separation abilities of complex samples have been demonstrated for microfluidic paper-based analytical devices (μPADs) [170]. The star-like configuration of these paper substrates generates a fast capillary-driven flow, capable of transporting both molecules and AuNRs into small detection spots of a cellulose microfiber. In addition, the modification of cellulose microfibers with oppositely charged polyelectrolytes enables separation of complex samples, thereby allowing the discrimination of different components. The combination of the μPADs with the SERS method enables detection at the attomolar level.

5.4 Filtration, centrifugation, and ultrasonication

Filtration was found to be an effective approach to functionalize commercially available filter paper [171]. The SERS performance of such substrates was assessed by probing R6G, melamine, and malathion, which were concentrated on SERS platforms using a filtration procedure (Fig. 2). The filtration-based SERS

technique enabled detection of 6.3 ppb melamine and 61.5 ppb malathion, with a low variability in the SERS signals. A nylon filter membrane decorated with AgNWs by filtration was successfully used for the extraction of contaminants in water [172]. The AgNWs-based filter membrane exhibits temporal stability under continuous laser irradiation, as well as uniformity and reproducibility of the SERS signal. The above investigation highlighted the advantages of solid-phase extraction (SPE) and SERS technologies for the rapid analysis of hazardous residues in water. Lin and coworkers have adopted a previously reported approach [114] to fabricate SERS substrates and use them for the detection of Rhodamine B (RB), both in aqueous solution and in chili powder [78]. The authors developed two methods for extracting RB from chili powder: centrifugation and ultrasonication. Using these procedures, they could complete the measurements within 10 min, with a detection limit of 1 μg/g. Prikhozhdenko et al. have used AgNPs to decorate chitosan nanofiber membranes via the silver mirror reaction [173, 174]. They studied the impact of the concentration of Tollens' reagent on the distribution of AgNPs, both in a group of nanofibers and in a single nanofiber. Two approaches for bacteria immobilization on SERS substrates were established. It was found that incubation promotes a stronger enhancement of microorganism signatures, with very low spot-to-spot variations in SERS spectra.

5.5 Integration with a microfluidic system

Gao and coworkers have studied the formation of irregular AgNPs, AuNP spheres, and nanorods in electrospun PVA nanofibers [175]. Multi-surface plasmon resonance (multi-SPR) nanofibrous films were tested for the detection of 4-mercaptobenzoic acid and 4-mercaptopyridine on a glass substrate, both in an organic solvent and in water. Subsequently, the multi-SPR nanofibrous films were integrated into a microfluidic chip and tested for the detection of R6G and 610-biotin (Fig. 3). The AuNR/PVA films exhibited excellent reproducibility, with signal variation of 8.3%–10% in the organic solvent and 16.9% in water.

5.6 Tailoring hydrophilicity/hydrophobicity and recovery of SERS substrates

Shao et al. have demonstrated the fabrication of locally hydrophilic hotspots on hydrophobic electrospun

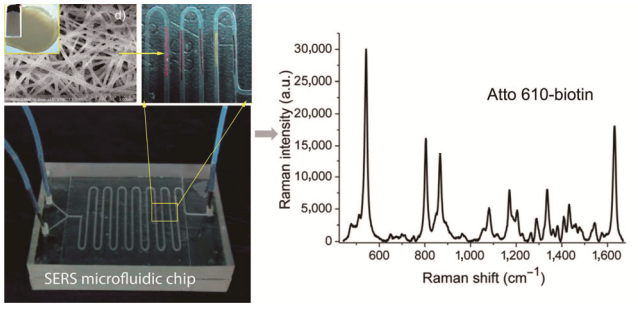

Figure 3 Photograph of a SERS microfluidic chip with several types of metal NP-doped PVA nanofiber films and SEM image of PVA membrane impregnated with AgNPs. SERS spectrum of Atto 610-biotin acquired by the SERS microfluidic chip. Reproduced with permission from Ref. [175], © The Royal Society of Chemistry 2014.

PLLA nanofiber films [176]. The high electrostatic affinity between cetyltrimethylammonium bromide (CTAB)-stabilized AuNRs and carboxylic groups on the surface of PLLA nanofibers results in the formation of hydrophilic areas on the hydrophobic substrate. The patches enable localization of analyte molecules on AuNR/PLLA films for highly sensitive, reproducible, and stable SERS detection. The authors demonstrated the detection of R6G and MG at extremely low concentrations (0.1 nM) and with excellent reproducibility (RSD ~ 8%). The above study demonstrated an efficient route to enhance the SERS sensitivity by tailoring the hydrophilicity/hydrophobicity of the hydrophilic substrates. Zhao et al. fabricated multifunctional electrospun nanofibrous felt made of PVP nanofibers, TiO_2, and Ag nanoparticles via the electroless plating method. Apart from the excellent SERS activity and sensitivity of the TiO_2/Ag nanofibrous felt, the samples could be cleaned and regenerated/recovered by UV irradiation in oxygen-saturated water.

The hybrid and UV-cleanable electrospun TiO_2/Ag nanofibrous felt is highly attractive as a recyclable substrate for SERS detection [77]. The electrospun PVA nanofibers containing AgNPs within a polymer matrix have been used both as antibacterial films and SERS-active substrates. The study of Ref. [77] highlighted the multifunctionality of hybrid AgNP/PVA nanofibrous films, which could broaden their applications. Jalaja and coworkers fabricated AgNP/polystyrene (PS) SERS substrates using electrospun porous PS mats [177]. The authors showed that trace amounts of

chemicals such as DNT and carbofuran on practical surfaces could be detected by simply wiping with wet flexible PS-SERS mats.

6 Conclusions and outlook

In this review, we discussed the latest achievements in the fabrication of low-cost flexible substrates for SERS sensing applications based on cellulose paper, electrospun polymer membranes, and textiles. A wide variety of methods and techniques have successfully been applied for the impregnation of each of these substrates with plasmonic nanoparticles. The 3D network formed by the nanofibers leads to a strong enhancement of the SERS signal, to levels comparable with those of rigid SERS platforms fabricated on silicon or glass.

In most cases, nanofibrous membranes demonstrated excellent reproducibility of the SERS signal along with low LODs. The excellent mechanical flexibility and bendability of these substrates open new opportunities for their application as swabs and dipsticks to collect trace amounts of analytes on rough surfaces. Moreover, all types of substrates can be formed into a specific shape, which facilitates the localization of molecules in small spots and therefore their SERS identification. Recent studies have shown that the combination of hydrophilic and hydrophobic components in nanofibrous membranes is very useful for SERS identification of highly diluted samples. In addition, the rational design of cleanable flexible nanofibrous membranes is a promising strategy for recyclable SERS measurements and multiple applications of SERS substrates.

However, despite numerous recent efforts to design, fabricate, and study flexible nanofibrous SERS substrates, several problems still need to be solved to enable their general use, beyond the laboratory stage. The uniform distribution of plasmonic nanoparticles on the flexible nanofibrous substrates, their long-term stability, and the resistance to degradation under various environmental conditions are important aspects to be addressed. We anticipate that the combination of LFIA and passive vertical flow membranes with the SERS method would enable ultrasensitive detection and simultaneous separation of the target analytes from biological fluids and, consequently, support the development of point-of-care diagnostics. In addition, the biocompatibility and biodegradability of the nanofibrous membranes are expected to support their future application as implantable or wearable SERS sensors. Another area of future research is the development of miniature devices capable of remotely monitoring the *in vivo* concentrations of drugs, hormones, and biomarkers operating with flexible SERS substrates.

Acknowledgements

The authors acknowledge Government of the Russian Federation (No. 14.Z50.31.0004) to support scientific research projects implemented under the supervision of leading scientists at Russian institutions). Ekaterina S. Prikhozhdenko acknowledges Deutscher Akademischer Austauschdienst (DAAD project no. 15.9970.2017/5.2).

References

[1] Fleischmann, M.; Hendra, P. J.; McQuillan, A. J. Raman spectra of pyridine adsorbed at a silver electrode. *Chem. Phys. Lett.* **1974**, *26*, 163–166.

[2] Jeanmaire, D. L.; Van Duyne, R. P. Surface Raman spectroelectrochemistry: Part I. Heterocyclic, aromatic, and aliphatic amines adsorbed on the anodized silver electrode. *J. Electroanal. Chem.* **1977**, *84*, 1–20.

[3] Albrecht, M. G.; Creighton, J. A. Anomalously intense Raman spectra of pyridine at a silver electrode. *J. Am. Chem. Soc.* **1977**, *99*, 5215–5217.

[4] Otto, A. Surface enhanced Raman scattering (SERS), what do we know? *Appl. Surf. Sci.* **1980**, *6*, 309–355.

[5] Moskovits, M. Surface-enhanced spectroscopy. *Rev. Mod. Phys.* **1985**, *57*, 783–826.

[6] Kneipp, K.; Hinzmann, G.; Fassler, D. Surface-enhanced Raman scattering of polymethine dyes on silver colloidal particles. *Chem. Phys. Lett.* **1983**, *99*, 503–506.

[7] Hildebrandt, P.; Stockburger, M. Surface-enhanced resonance Raman spectroscopy of Rhodamine 6G adsorbed on colloidal silver. *J. Phys. Chem.* **1984**, *88*, 5935–5944.

[8] Kneipp, K.; Wang, Y.; Kneipp, H.; Itzkan, I.; Dasari, R. R.; Feld, M. S. Population pumping of excited vibrational states by spontaneous surface-enhanced Raman scattering. *Phys. Rev. Lett.* **1996**, *76*, 2444–2447.

[9] Safonov, V. P.; Shalaev, V. M.; Markel, V. A.; Danilova, Y. E.; Lepeshkin, N. N.; Kim, W.; Rautian, S. G.; Armstrong, R. L. Spectral dependence of selective photomodification in fractal aggregates of colloidal particles. *Phys. Rev. Lett.* **1998**, *80*, 1102–1105.

[10] Zhang, G. N.; Qu, G.; Chen, Y.; Shen, A. G.; Xie, W.; Zhou, X. D.; Hu, J. M. Controlling carbon encapsulation of gold nanoaggregates as highly sensitive and spectrally stable SERS tags for live cell imaging. *J. Mater. Chem. B* **2013**, *1*, 4364–4369.

[11] Shiohara, A.; Wang, Y. S.; Liz-Marzán, L. M. Recent approaches toward creation of hot spots for SERS detection. *J. Photochem. Photobiol. C Photochem. Rev.* **2014**, *21*, 2–25.

[12] Nie, S. M.; Emory, S. R. Probing single molecules and single nanoparticles by surface-enhanced Raman scattering. *Science* **1997**, *275*, 1102–1106.

[13] Kneipp, K.; Wang, Y.; Kneipp, H.; Perelman, L. T.; Itzkan, I.; Dasari, R. R.; Feld, M. S. Single molecule detection using surface-enhanced Raman scattering (SERS). *Phys. Rev. Lett.* **1997**, *78*, 1667–1670.

[14] Wang, Y.; Irudayaraj, J. Surface-enhanced Raman spectroscopy at single-molecule scale and its implications in biology. *Philos. Trans. R. Soc. B Biol. Sci.* **2012**, *368*, 20120026.

[15] Giner-Casares, J. J.; Liz-Marzán, L. M. Plasmonic nanoparticles in 2D for biological applications: Toward active multipurpose platforms. *Nano Today* **2014**, *9*, 365–377.

[16] Luo, S.-C.; Sivashanmugan, K.; Liao, J.-D.; Yao, C.-K.; Peng, H.-C. Nanofabricated SERS-active substrates for single-molecule to virus detection *in vitro*: A review. *Biosens. Bioelectron.* **2014**, *61*, 232–240.

[17] Xie, W.; Walkenfort, B.; Schlücker, S. Label-free SERS monitoring of chemical reactions catalyzed by small gold nanoparticles using 3D plasmonic superstructures. *J. Am. Chem. Soc.* **2013**, *135*, 1657–1660.

[18] Cui, Q. L.; Shen, G. Z.; Yan, X. H.; Li, L. D.; Möhwald, H.; Bargheer, M. Fabrication of Au@Pt multibranched nanoparticles and their application to *in situ* SERS monitoring. *ACS Appl. Mater. Interfaces* **2014**, *6*, 17075–17081.

[19] Thomas, M.; Mühlig, S.; Deckert-Gaudig, T.; Rockstuhl, C.; Deckert, V.; Marquetand, P. Distinguishing chemical and electromagnetic enhancement in surface-enhanced Raman spectra: The case of para-nitrothiophenol. *J. Raman Spectrosc.* **2013**, *44*, 1497–1505.

[20] Muniz-Miranda, M. Application of the SERS spectroscopy to the study of catalytic reactions by means of mono and bimetallic nanoparticles. *J. Anal. Bioanal. Tech.* **2015**, *6*, 286.

[21] Wang, Y. L.; Seebald, J. L.; Szeto, D. P.; Irudayaraj, J. Biocompatibility and biodistribution of surface-enhanced Raman scattering nanoprobes in zebrafish embryos: *In vivo* and multiplex imaging. *ACS Nano* **2010**, *4*, 4039–4053.

[22] Vo-Dinh, T.; Wang, H.-N.; Scaffidi, J. Plasmonic nanoprobes for SERS biosensing and bioimaging. *J. Biophotonics* **2009**, *3*, 89–102.

[23] Giner-Casares, J. J.; Henriksen-Lacey, M.; Coronado-Puchau, M.; Liz-Marzán, L. M. Inorganic nanoparticles for biomedicine: Where materials scientists meet medical research. *Mater. Today* **2016**, *19*, 19–28.

[24] Harmsen, S.; Huang, R. M.; Wall, M. A.; Karabeber, H.; Samii, J. M.; Spaliviero, M.; White, J. R.; Monette, S.; O'Connor, R.; Pitter, K. L. et al. Surface-enhanced resonance Raman scattering nanostars for high-precision cancer imaging. *Sci. Transl. Med.* **2015**, *7*, 271ra7.

[25] Wang, X.; Qian, X. M.; Beitler, J. J.; Chen, Z. G.; Khuri, F. R.; Lewis, M. M.; Shin, H. J. C.; Nie, S. M.; Shin, D. M. Detection of circulating tumor cells in human peripheral blood using surface-enhanced Raman scattering nanoparticles. *Cancer Res.* **2011**, *71*, 1526–1532.

[26] Karabeber, H.; Huang, R. M.; Iacono, P.; Samii, J. M.; Pitter, K. L.; Holland, E. C.; Kircher, M. F. Guiding brain tumor resection using surface-enhanced Raman scattering nanoparticles and a hand-held Raman scanner. *ACS Nano* **2014**, *8*, 9755–9766.

[27] Fan, M. K.; Andrade, G. F. S.; Brolo, A. G. A review on the fabrication of substrates for surface enhanced Raman spectroscopy and their applications in analytical chemistry. *Anal. Chim. Acta* **2011**, *693*, 7–25.

[28] Polavarapu, L.; Liz-Marzán, L. M. Towards low-cost flexible substrates for nanoplasmonic sensing. *Phys. Chem. Chem. Phys.* **2013**, *15*, 5288–5300.

[29] Haynes, C. L.; Van Duyne, R. P. Nanosphere lithography: A versatile nanofabrication tool for studies of size-dependent nanoparticle optics. *J. Phys. Chem. B* **2001**, *105*, 5599–5611.

[30] Schmidt, M. S.; Hübner, J.; Boisen, A. Large area fabrication of leaning silicon nanopillars for surface enhanced Raman spectroscopy. *Adv. Mater.* **2011**, *24*, OP11–OP18.

[31] Leordean, C.; Gabudean, A.-M.; Canpean, V.; Astilean, S. Easy and cheap fabrication of ordered pyramidal-shaped plasmonic substrates for detection and quantitative analysis using surface-enhanced Raman spectroscopy. *Analyst* **2013**, *138*, 4975–4981.

[32] Merk, V.; Kneipp, J.; Leosson, K. Gap size reduction and increased SERS enhancement in lithographically patterned nanoparticle arrays by templated growth. *Adv. Opt. Mater.* **2013**, *1*, 313–318.

[33] Saracut, V.; Giloan, M.; Gabor, M.; Astilean, S.; Farcau, C. Polarization-sensitive linear plasmonic nanostructures via colloidal lithography with uniaxial colloidal arrays. *ACS Appl. Mater. Interfaces* **2013**, *5*, 1362–1369.

[34] Keating, M.; Song, S.; Wei, G.; Graham, D.; Chen, Y.; Placido, F. Ordered silver and copper nanorod arrays for enhanced Raman scattering created via guided oblique angle deposition on polymer. *J. Phys. Chem. C* **2014**, *118*, 4878–4884.

[35] Chen, B. S.; Meng, G. W.; Zhou, F.; Huang, Q.; Zhu, C. H.;

Hu, X. Y.; Kong, M. G. Ordered arrays of Au-nanobowls loaded with Ag-nanoparticles as effective SERS substrates for rapid detection of PCBs. *Nanotechnology* **2014**, *25*, 145605.

[36] Ou, F. S.; Hu, M.; Naumov, I.; Kim, A.; Wu, W.; Bratkovsky, A. M.; Li, X. M.; Williams, R. S.; Li, Z. Y. Hot-spot engineering in polygonal nanofinger assemblies for surface enhanced Raman spectroscopy. *Nano Lett.* **2011**, *11*, 2538–2542.

[37] Wu, H.-Y.; Choi, C. J.; Cunningham, B. T. Plasmonic nanogap-enhanced Raman scattering using a resonant nanodome array. *Small* **2012**, *8*, 2878–2885.

[38] Yang, J.; Palla, M.; Bosco, F. G.; Rindzevicius, T.; Alstrøm, T. S.; Schmidt, M. S.; Boisen, A.; Ju, J. Y.; Lin, Q. Surface-enhanced Raman spectroscopy based quantitative bioassay on aptamer-functionalized nanopillars using large-area Raman mapping. *ACS Nano* **2013**, *7*, 5350–5359.

[39] Wu, K. Y.; Rindzevicius, T.; Schmidt, M. S.; Mogensen, K. B.; Hakonen, A.; Boisen, A. Wafer-scale leaning silver nanopillars for molecular detection at ultra-low concentrations. *J. Phys. Chem. C* **2015**, *119*, 2053–2062.

[40] Serrano-Montes, A. B.; Jimenez de Aberasturi, D.; Langer, J.; Giner-Casares, J. J.; Scarabelli, L.; Herrero, A.; Liz-Marzán, L. M. A general method for solvent exchange of plasmonic nanoparticles and self-assembly into SERS-active monolayers. *Langmuir* **2015**, *31*, 9205–9213.

[41] Hu, X. G.; Cheng, W. L.; Wang, T.; Wang, Y. L.; Wang, E. K.; Dong, S. J. Fabrication, characterization, and application in SERS of self-assembled polyelectrolyte-gold nanorod multilayered films. *J. Phys. Chem. B* **2005**, *109*, 19385–19389.

[42] Pazos-Pérez, N.; Wagner, C. S.; Romo-Herrera, J. M.; Liz-Marzán, L. M.; García de Abajo, F. J.; Wittemann, A.; Fery, A.; Álvarez-Puebla, R. A. Organized plasmonic clusters with high coordination number and extraordinary enhancement in surface-enhanced Raman scattering (SERS). *Angew. Chem., Int. Ed.* **2012**, *51*, 12688–12693.

[43] Leiterer, C.; Zopf, D.; Seise, B.; Jahn, F.; Weber, K.; Popp, J.; Cialla-May, D.; Fritzsche, W. Fast self-assembly of silver nanoparticle monolayer in hydrophobic environment and its application as SERS substrate. *J. Nanoparticle Res.* **2014**, *16*, 2467.

[44] Lee, Y. H.; Lee, C. K.; Tan, B. R.; Rui Tan, J. M.; Phang, I. Y.; Ling, X. Y. Using the Langmuir–Schaefer technique to fabricate large-area dense SERS-active Au nanoprism monolayer films. *Nanoscale* **2013**, *5*, 6404–6412.

[45] La Porta, A.; Grzelczak, M.; Liz-Marzán, L. M. Gold nanowire forests for SERS detection. *ChemistryOpen* **2014**, *3*, 146–151.

[46] Abdelsalam, M. E.; Mahajan, S.; Bartlett, P. N.; Baumberg, J. J.; Russell, A. E. SERS at structured palladium and platinum surfaces. *J. Am. Chem. Soc.* **2007**, *129*, 7399–7406.

[47] Khanadeev, V. A.; Khlebtsov, B. N.; Klimova, S. A.; Tsvetkov, M. Y.; Bagratashvili, V. N.; Sukhorukov, G. B.; Khlebtsov, N. G. Large-scale high-quality 2D silica crystals: Dip-drawing formation and decoration with gold nanorods and nanospheres for SERS analysis. *Nanotechnology* **2014**, *25*, 405602.

[48] Pazos-Pérez, N.; Ni, W. H.; Schweikart, A.; Álvarez-Puebla, R. A.; Fery, A.; Liz-Marzán, L. M. Highly uniform SERS substrates formed by wrinkle-confined drying of gold colloids. *Chem. Sci.* **2010**, *1*, 174–178.

[49] Lee, J.; Seo, J.; Kim, D.; Shin, S.; Lee, S.; Mahata, C.; Lee, H.-S.; Min, B.-W.; Lee, T. Capillary force-induced glue-free printing of Ag nanoparticle arrays for highly sensitive SERS substrates. *ACS Appl. Mater. Interfaces* **2014**, *6*, 9053–9060.

[50] Kneipp, J.; Kneipp, H.; McLaughlin, M.; Brown, D.; Kneipp, K. *In vivo* molecular probing of cellular compartments with gold nanoparticles and nanoaggregates. *Nano Lett.* **2006**, *6*, 2225–2231.

[51] Radziuk, D.; Schuetz, R.; Masic, A.; Moehwald, H. Chemical imaging of live fibroblasts by SERS effective nanofilm. *Phys. Chem. Chem. Phys.* **2014**, *16*, 24621–24634.

[52] Yashchenok, A.; Masic, A.; Gorin, D.; Shim, B. S.; Kotov, N. A.; Fratzl, P.; Möhwald, H.; Skirtach, A. Nanoengineered colloidal probes for Raman-based detection of biomolecules inside living cells. *Small* **2013**, *9*, 351–356.

[53] Stetciura, I. Y.; Yashchenok, A. M.; Masic, A.; Lyubin, E. V.; Inozemtseva, O. A.; Drozdova, M. G.; Markvichova, E. A.; Khlebtsov, B. N.; Fedyanin, A. A.; Sukhorukov, G. B. et al. Composite SERS-based satellites navigated by optical tweezers for single cell analysis. *Analyst* **2015**, *140*, 4981–4986.

[54] Ahijado-Guzmán, R.; Gómez-Puertas, P.; Álvarez-Puebla, R. A.; Rivas, G.; Liz-Marzán, L. M. Surface-enhanced Raman scattering-based detection of the interactions between the essential cell division FtsZ protein and bacterial membrane elements. *ACS Nano* **2012**, *6*, 7514–7520.

[55] Xu, L. G.; Kuang, H.; Xu, C. L.; Ma, W.; Wang, L. B.; Kotov, N. A. Regiospecific plasmonic assemblies for *in situ* Raman spectroscopy in live cells. *J. Am. Chem. Soc.* **2012**, *134*, 1699–1709.

[56] Xu, L. J.; Lei, Z. C.; Li, J. X.; Zong, C.; Yang, C. J.; Ren, B. Label-free surface-enhanced Raman spectroscopy detection of DNA with single-base sensitivity. *J. Am. Chem. Soc.* **2015**, *137*, 5149–5154.

[57] Xu, L.-J.; Zong, C.; Zheng, X.-S.; Hu, P.; Feng, J.-M.; Ren, B. Label-free detection of native proteins by surface-enhanced Raman spectroscopy using iodide-modified nanoparticles. *Anal. Chem.* **2014**, *86*, 2238–2245.

[58] Bodelón, G.; Montes-García, V.; López-Puente, V.; Hill, E. H.; Hamon, C.; Sanz-Ortiz, M. N.; Rodal-Cedeira, S.; Costas, C.;

Celiksoy, S.; Pérez-Juste, I. et al. Detection and imaging of quorum sensing in pseudomonas aeruginosa biofilm communities by surface-enhanced resonance Raman scattering. *Nat. Mater.* **2016**, *15*, 1203–1211.

[59] De Angelis, F.; Gentile, F.; Mecarini, F.; Das, G.; Moretti, M.; Candeloro, P.; Coluccio, M. L.; Cojoc, G.; Accardo, A.; Liberale, C. et al. Breaking the diffusion limit with super-hydrophobic delivery of molecules to plasmonic nanofocusing SERS structures. *Nat. Photonics* **2011**, *5*, 682–687.

[60] Zhai, W.-L.; Li, D.-W.; Qu, L.-L.; Fossey, J. S.; Long, Y.-T. Multiple depositions of Ag nanoparticles on chemically modified agarose films for surface-enhanced Raman spectroscopy. *Nanoscale* **2012**, *4*, 137–142.

[61] Tian, L. M.; Luan, J. Y.; Liu, K.-K.; Jiang, Q. S.; Tadepalli, S.; Gupta, M. K.; Naik, R. R.; Singamaneni, S. Plasmonic biofoam: A versatile optically active material. *Nano Lett.* **2016**, *16*, 609–616.

[62] Tian, L. M.; Jiang, Q. S.; Liu, K.-K.; Luan, J. Y.; Naik, R. R.; Singamaneni, S. Bacterial nanocellulose-based flexible surface enhanced Raman scattering substrate. *Adv. Mater. Interfaces* **2016**, *3*, 1600214.

[63] Gong, Z. J.; Wang, C. C.; Wang, C.; Tang, C. Y.; Cheng, F. S.; Du, H. J.; Fan, M. K.; Brolo, A. G. A silver nanoparticle embedded hydrogel as a substrate for surface contamination analysis by surface-enhanced Raman scattering. *Analyst* **2014**, *139*, 5283–5289.

[64] Gong, Z. J.; Wang, C. C.; Pu, S.; Wang, C.; Cheng, F. S.; Wang, Y. H.; Fan, M. K. Rapid and direct detection of illicit dyes on tainted fruit peel using a PVA hydrogel surface enhanced Raman scattering substrate. *Anal. Methods* **2016**, *8*, 4816–4820.

[65] Park, M.; Chang, H.; Jeong, D. H.; Hyun, J. Spatial deformation of nanocellulose hydrogel enhances SERS. *BioChip J.* **2013**, *7*, 234–241.

[66] Park, S.-G.; Ahn, M.-S.; Oh, Y.-J.; Kang, M.; Jeong, Y.; Jeong, K.-H. Nanoplasmonic biopatch for *in vivo* surface enhanced Raman spectroscopy. *BioChip J.* **2014**, *8*, 289–294.

[67] Fernández-López, C.; Polavarapu, L.; Solís, D. M.; Taboada, J. M.; Obelleiro, F.; Contreras-Cáceres, R.; Pastoriza-Santos, I.; Pérez-Juste, J. Gold nanorod–pNIPAM hybrids with reversible plasmon coupling: Synthesis, modeling, and SERS properties. *ACS Appl. Mater. Interfaces* **2015**, *7*, 12530–12538.

[68] Álvarez-Puebla, R. A.; Contreras-Cáceres, R.; Pastoriza-Santos, I.; Pérez-Juste, J.; Liz-Marzán, L. M. Au@pNIPAM colloids as molecular traps for surface-enhanced, spectroscopic, ultra-sensitive analysis. *Angew. Chem., Int. Ed.* **2009**, *48*, 138–143.

[69] Contreras-Cáceres, R.; Abalde-Cela, S.; Guardia-Girós, P.; Fernández-Barbero, A.; Pérez-Juste, J.; Álvarez-Puebla, R. A.; Liz-Marzán, L. M. Multifunctional microgel magnetic/optical traps for SERS ultradetection. *Langmuir* **2011**, *27*, 4520–4525.

[70] Aldeanueva-Potel, P.; Faoucher, E.; Álvarez-Puebla, R. A.; Liz-Marzán, L. M.; Brust, M. Recyclable molecular trapping and SERS detection in silver-loaded agarose gels with dynamic hot spots. *Anal. Chem.* **2009**, *81*, 9233–9238.

[71] Lee, S. J.; Moskovits, M. Remote sensing by plasmonic transport. *J. Am. Chem. Soc.* **2012**, *134*, 11384–11387.

[72] Qian, X. M.; Peng, X.-H.; Ansari, D. O.; Yin-Goen, Q.; Chen, G. Z.; Shin, D. M.; Yang, L.; Young, A. N.; Wang, M. D.; Nie, S. M. *In vivo* tumor targeting and spectroscopic detection with surface-enhanced Raman nanoparticle tags. *Nat. Biotechnol.* **2008**, *26*, 83–90.

[73] Sanles-Sobrido, M.; Exner, W.; Rodríguez-Lorenzo, L.; Rodríguez-González, B.; Correa-Duarte, M. A.; Álvarez-Puebla, R. A.; Liz-Marzán, L. M. Design of SERS-encoded, submicron, hollow particles through confined growth of encapsulated metal nanoparticles. *J. Am. Chem. Soc.* **2009**, *131*, 2699–2705.

[74] Samanta, A.; Maiti, K. K.; Soh, K. S.; Liao, X. J.; Vendrell, M.; Dinish, U. S.; Yun, S. W.; Bhuvaneswari, R.; Kim, H.; Rautela, S. et al. Ultrasensitive near-infrared Raman reporters for SERS-based *in vivo* cancer detection. *Angew. Chem., Int. Ed.* **2011**, *50*, 6089–6092.

[75] Samanta, A.; Das, R. K.; Park, S. J.; Maiti, K. K.; Chang, Y. T. Multiplexing SERS nanotags for the imaging of differentiated mouse embryonic stem cells (mESC) and detection of teratoma *in vivo*. *Am. J. Nucl. Med. Mol. Imaging* **2014**, *4*, 114–124.

[76] Gandra, N.; Singamaneni, S. Bilayered Raman-intense gold nanostructures with hidden tags (BRIGHTs) for high-resolution bioimaging. *Adv. Mater.* **2013**, *25*, 1022–1027.

[77] Zhao, Y.; Sun, L.; Xi, M.; Feng, Q.; Jiang, C. Y.; Fong, H. Electrospun TiO_2 nanofelt surface-decorated with Ag nanoparticles as sensitive and UV-cleanable substrate for surface enhanced Raman scattering. *ACS Appl. Mater. Interfaces* **2014**, *6*, 5759–5767.

[78] Lin, S.; Hasi, W.-L.-J.; Lin, X.; Han, S.; Lou, X.-T.; Yang, F.; Lin, D.-Y.; Lu, Z.-W. Rapid and sensitive SERS method for determination of Rhodamine B in chili powder with paper-based substrates. *Anal. Methods* **2015**, *7*, 5289–5294.

[79] Khlebtsov, B.; Pylaev, T.; Khanadeev, V.; Bratashov, D.; Khlebtsov, N. Quantitative and multiplex dot-immunoassay using gap-enhanced Raman tags. *RSC Adv.* **2017**, *7*, 40834–40841.

[80] Yang, X.; Gu, C.; Qian, F.; Li, Y.; Zhang, J. Z. Highly sensitive detection of proteins and bacteria in aqueous

solution using surface-enhanced Raman scattering and optical fibers. *Anal. Chem.* **2011**, *83*, 5888–5894.

[81] Dinish, U. S.; Fu, C. Y.; Soh, K. S.; Ramaswamy, B.; Kumar, A.; Olivo, M. Highly sensitive SERS detection of cancer proteins in low sample volume using hollow core photonic crystal fiber. *Biosens. Bioelectron.* **2012**, *33*, 293–298.

[82] Zavaleta, C. L.; Garai, E.; Liu, J. T. C.; Sensarn, S.; Mandella, M. J.; Van de Sompel, D.; Friedland, S.; Van Dam, J.; Contag, C. H.; Gambhir, S. S. A Raman-based endoscopic strategy for multiplexed molecular imaging. *Proc. Natl. Acad. Sci. USA* **2013**, *110*, 10062–10063.

[83] Martinez, A. W.; Phillips, S. T.; Whitesides, G. M.; Carrilho, E. Diagnostics for the developing world: Microfluidic paper-based analytical devices. *Anal. Chem.* **2010**, *82*, 3–10.

[84] Parolo, C.; Merkoçi, A. Paper-based nanobiosensors for diagnostics. *Chem. Soc. Rev.* **2013**, *42*, 450–457.

[85] Jia, H. Y.; Wang, J.; Zhang, X. Y.; Wang, Y. P. Pen-writing polypyrrole arrays on paper for versatile cheap sensors. *ACS Macro Lett.* **2014**, *3*, 86–90.

[86] Jason, N. N.; Shen, W.; Cheng, W. L. Copper nanowires as conductive ink for low-cost draw-on electronics. *ACS Appl. Mater. Interfaces* **2015**, *7*, 16760–16766.

[87] Kumar, S.; Bhat, V.; Vinoy, K. J.; Santhanam, V. Using an office inkjet printer to define the formation of copper films on paper. *IEEE Trans. Nanotechnol.* **2014**, *13*, 160–164.

[88] Tseng, S.-C.; Yu, C.-C.; Wan, D. H.; Chen, H.-L.; Wang, L. A.; Wu, M.-C.; Su, W.-F.; Han, H.-C.; Chen, L.-C. Eco-friendly plasmonic sensors: Using the photothermal effect to prepare metal nanoparticle-containing test papers for highly sensitive colorimetric detection. *Anal. Chem.* **2012**, *84*, 5140–5145.

[89] Russo, A.; Ahn, B. Y.; Adams, J. J.; Duoss, E. B.; Bernhard, J. T.; Lewis, J. A. Pen-on-paper flexible electronics. *Adv. Mater.* **2011**, *23*, 3426–3430.

[90] Kim, Y. T.; Chen, Y. C.; Choi, J. Y.; Kim, W.-J.; Dae, H.-M.; Jung, J.; Seo, T. S. Integrated microdevice of reverse transcription-polymerase chain reaction with colorimetric immunochromatographic detection for rapid gene expression analysis of influenza A H1N1 virus. *Biosens. Bioelectron.* **2012**, *33*, 88–94.

[91] He, Y. Q.; Zhang, S. Q.; Zhang, X. B.; Baloda, M.; Gurung, A. S.; Xu, H.; Zhang, X. J.; Liu, G. D. Ultrasensitive nucleic acid biosensor based on enzyme-gold nanoparticle dual label and lateral flow strip biosensor. *Biosens. Bioelectron.* **2011**, *26*, 2018–2024.

[92] Li, C. Z.; Vandenberg, K.; Prabhulkar, S.; Zhu, X. N.; Schneper, L.; Methee, K.; Rosser, C. J.; Almeide, E. Paper based point-of-care testing disc for multiplex whole cell bacteria analysis. *Biosens. Bioelectron.* **2011**, *26*, 4342–4348.

[93] Martinez, A. W.; Phillips, S. T.; Whitesides, G. M. Three-dimensional microfluidic devices fabricated in layered paper and tape. *Proc. Natl. Acad. Sci. USA* **2008**, *105*, 19606–19611.

[94] Carrilho, E.; Phillips, S. T.; Vella, S. J.; Martinez, A. W.; Whitesides, G. M. Paper microzone plates. *Anal. Chem.* **2009**, *81*, 5990–5998.

[95] Shin, K.-Y.; Hong, J.-Y.; Jang, J. Micropatterning of graphene sheets by inkjet printing and its wideband dipole-antenna application. *Adv. Mater.* **2011**, *23*, 2113–2118.

[96] Kamyshny, A.; Magdassi, S. Conductive nanomaterials for printed electronics. *Small* **2014**, *10*, 3515–3535.

[97] Yao, B.; Yuan, L. Y.; Xiao, X.; Zhang, J.; Qi, Y. Y.; Zhou, J.; Zhou, J.; Hu, B.; Chen, W. Paper-based solid-state supercapacitors with pencil-drawing graphite/polyaniline networks hybrid electrodes. *Nano Energy* **2013**, *2*, 1071–1078.

[98] Schmucker, A. L.; Tadepalli, S.; Liu, K.-K.; Sullivan, C. J.; Singamaneni, S.; Naik, R. R. Plasmonic paper: A porous and flexible substrate enabling nanoparticle-based combinatorial chemistry. *RSC Adv.* **2016**, *6*, 4136–4144.

[99] Ross, M. B.; Ashley, M. J.; Schmucker, A. L.; Singamaneni, S.; Naik, R. R.; Schatz, G. C.; Mirkin, C. A. Structure–function relationships for surface-enhanced Raman spectroscopy-active plasmonic paper. *J. Phys. Chem. C* **2016**, *120*, 20789–20797.

[100] Tian, L. M.; Morrissey, J. J.; Kattumenu, R.; Gandra, N.; Kharasch, E. D.; Singamaneni, S. Bioplasmonic paper as a platform for detection of kidney cancer biomarkers. *Anal. Chem.* **2012**, *84*, 9928–9934.

[101] Polavarapu, L.; La Porta, A.; Novikov, S. M.; Coronado-Puchau, M.; Liz-Marzán, L. M. Pen-on-paper approach toward the design of universal surface enhanced Raman scattering substrates. *Small* **2014**, *10*, 3065–3071.

[102] Tran, C. D. Subnanogram detection of dyes on filter paper by surface-enhanced Raman scattering spectrometry. *Anal. Chem.* **1984**, *56*, 824–826.

[103] Lee, C. H.; Hankus, M. E.; Tian, L. M.; Pellegrino, P. M.; Singamaneni, S. Highly sensitive surface enhanced Raman scattering substrates based on filter paper loaded with plasmonic nanostructures. *Anal. Chem.* **2011**, *83*, 8953–8958.

[104] Ngo, Y. H.; Li, D.; Simon, G. P.; Garnier, G. Gold nanoparticle–paper as a three-dimensional surface enhanced Raman scattering substrate. *Langmuir* **2012**, *28*, 8782–8790.

[105] Ngo, Y. H.; Li, D.; Simon, G. P.; Garnier, G. Effect of cationic polyacrylamides on the aggregation and SERS performance of gold nanoparticles-treated paper. *J. Colloid Interface Sci.* **2013**, *392*, 237–246.

[106] Hasi, W.-L.-J.; Lin, S.; Lin, X.; Lou, X.-T.; Yang, F.; Lin, D.-Y.; Lu, Z.-W. Rapid fabrication of self-assembled interfacial film decorated filter paper as an excellent surface-enhanced Raman scattering substrate. *Anal. Methods*

2014, *6*, 9547–9553.

[107] Zhang, W.; Li, B. W.; Chen, L. X.; Wang, Y. Q.; Gao, D. X.; Ma, X. H.; Wu, A. G. Brushing, a simple way to fabricate SERS active paper substrates. *Anal. Methods* **2014**, *6*, 2066–2071.

[108] Cheng, M.-L.; Tsai, B.-C.; Yang, J. Silver nanoparticle-treated filter paper as a highly sensitive surface-enhanced Raman scattering (SERS) substrate for detection of tyrosine in aqueous solution. *Anal. Chim. Acta* **2011**, *708*, 89–96.

[109] Kim, W.; Lee, J.-C.; Shin, J.-H.; Jin, K.-H.; Park, H.-K.; Choi, S. Instrument-free synthesizable fabrication of label-free optical biosensing paper strips for the early detection of infectious keratoconjunctivitides. *Anal. Chem.* **2016**, *88*, 5531–5537.

[110] Joshi, P.; Santhanam, V. Paper-based SERS active substrates on demand. *RSC Adv.* **2016**, *6*, 68545–68552.

[111] Qu, L.-L.; Li, D.-W.; Xue, J.-Q.; Zhai, W.-L.; Fossey, J. S.; Long, Y.-T. Batch fabrication of disposable screen printed SERS arrays. *Lab Chip* **2012**, *12*, 876–881.

[112] Zheng, G. C.; Polavarapu, L.; Liz-Marzán, L. M.; Pastoriza-Santos, I.; Pérez-Juste, J. Gold nanoparticle-loaded filter paper: A recyclable dip-catalyst for real-time reaction monitoring by surface enhanced Raman scattering. *Chem. Commun.* **2015**, *51*, 4572–4575.

[113] He, S.; Chua, J.; Tan, E. K. M.; Kah, J. C. Y. Optimizing the SERS enhancement of a facile gold nanostar immobilized paper-based SERS substrate. *RSC Adv.* **2017**, *7*, 16264–16272.

[114] Mehn, D.; Morasso, C.; Vanna, R.; Bedoni, M.; Prosperi, D.; Gramatica, F. Immobilised gold nanostars in a paper-based test system for surface-enhanced Raman spectroscopy. *Vib. Spectrosc.* **2013**, *68*, 45–50.

[115] Yu, W. W.; White, I. M. Inkjet printed surface enhanced Raman spectroscopy array on cellulose paper. *Anal. Chem.* **2010**, *82*, 9626–9630.

[116] Hoppmann, E. P.; Yu, W. W.; White, I. M. Highly sensitive and flexible inkjet printed SERS sensors on paper. *Methods* **2013**, *63*, 219–224.

[117] Liao, W.-J.; Roy, P. K.; Chattopadhyay, S. An ink-jet printed, surface enhanced Raman scattering paper for food screening. *RSC Adv.* **2014**, *4*, 40487–40493.

[118] Zhang, R.; Xu, B.-B.; Liu, X.-Q.; Zhang, Y.-L.; Xu, Y.; Chen, Q.-D.; Sun, H.-B. Highly efficient SERS test strips. *Chem. Commun.* **2012**, *48*, 5913–5915.

[119] Fan, M. K.; Zhang, Z. G.; Hu, J. M.; Cheng, F. S.; Wang, C.; Tang, C. Y.; Lin, J. H.; Brolo, A. G.; Zhan, H. Q. Ag decorated sandpaper as flexible SERS substrate for direct swabbing sampling. *Mater. Lett.* **2014**, *133*, 57–59.

[120] Chen, J.; Wu, X. M.; Huang, Y.-W.; Zhao, Y. P. Detection of *E. coli* using SERS active filters with silver nanorod array. *Sensors Actuators B Chem.* **2014**, *191*, 485–490.

[121] Zhu, Y. Q.; Li, M. Q.; Yu, D. Y.; Yang, L. B. A novel paper rag as "D-SERS" substrate for detection of pesticide residues at various peels. *Talanta* **2014**, *128*, 117–124.

[122] Yu, C.-C.; Chou, S.-Y.; Tseng, Y.-C.; Tseng, S.-C.; Yen, Y.-T.; Chen, H.-L. Single-shot laser treatment provides quasi-three-dimensional paper-based substrates for SERS with attomolar sensitivity. *Nanoscale* **2015**, *7*, 1667–1677.

[123] Ramakrishna, S.; Fujihara, K.; Teo, W.-E.; Yong, T.; Ma, Z. W.; Ramaseshan, R. Electrospun nanofibers: Solving global issues. *Mater. Today* **2006**, *9*, 40–50.

[124] Inozemtseva, O. A.; Salkovskiy, Y. E.; Severyukhina, A. N.; Vidyasheva, I. V.; Petrova, N. V.; Metwally, H. A.; Stetciura, I. Y.; Gorin, D. A. Electrospinning of functional materials for biomedicine and tissue engineering. *Russ. Chem. Rev.* **2015**, *84*, 251–274.

[125] Martins, A.; Araújo, J. V.; Reis, R. L.; Neves, N. M. Electrospun nanostructured scaffolds for tissue engineering applications. *Nanomedicine* **2007**, *2*, 929–942.

[126] Chen, C.; Tang, Y.; Vlahovic, B.; Yan, F. Electrospun polymer nanofibers decorated with noble metal nanoparticles for chemical sensing. *Nanoscale Res. Lett.* **2017**, *12*, 451.

[127] He, D.; Hu, B.; Yao, Q. F.; Wang, K.; Yu, S. H. Large-scale synthesis of flexible free-standing SERS substrates with high sensitivity: Electrospun PVA nanofibers embedded with controlled alignment of silver nanoparticles. *ACS Nano* **2009**, *3*, 3993–4002.

[128] Zhang, C.-L.; Lv, K.-P.; Cong, H.-P.; Yu, S.-H. Controlled assemblies of gold nanorods in PVA nanofiber matrix as flexible free-standing SERS substrates by electrospinning. *Small* **2012**, *8*, 648–653.

[129] Bao, Y.; Lai, C. L.; Zhu, Z. T.; Fong, H.; Jiang, C. Y. SERS-active silver nanoparticles on electrospun nanofibers facilitated via oxygen plasma etching. *RSC Adv.* **2013**, *3*, 8998–9004.

[130] Zhang, L. F.; Gong, X.; Bao, Y.; Zhao, Y.; Xi, M.; Jiang, C. Y.; Fong, H. Electrospun nanofibrous membranes surface-decorated with silver nanoparticles as flexible and active/sensitive substrates for surface-enhanced Raman scattering. *Langmuir* **2012**, *28*, 14433–14440.

[131] Lee, C. H.; Tian, L. M.; Abbas, A.; Kattumenu, R.; Singamaneni, S. Directed assembly of gold nanorods using aligned electrospun polymer nanofibers for highly efficient SERS substrates. *Nanotechnology* **2011**, *22*, 275311.

[132] Qian, Y. W.; Meng, G. W.; Huang, Q.; Zhu, C. H.; Huang, Z. L.; Sun, K. X.; Chen, B. Flexible membranes of Ag-nanosheet-grafted polyamide-nanofibers as effective 3D SERS substrates. *Nanoscale* **2014**, *6*, 4781–4788.

[133] Severyukhina, A. N.; Parakhonskiy, B. V.; Prikhozhdenko, E. S.; Gorin, D. A.; Sukhorukov, G. B.; Möhwald, H.;

Yashchenok, A. M. Nanoplasmonic chitosan nanofibers as effective SERS substrate for detection of small molecules. *ACS Appl. Mater. Interfaces* **2015**, *7*, 15466–15473.

[134] Yang, H.; Huang, C. Z. Polymethacrylic acid–facilitated nanofiber matrix loading Ag nanoparticles for SERS measurements. *RSC Adv.* **2014**, *4*, 38783–38790.

[135] Yang, T.; Yang, H.; Zhen, S. J.; Huang, C. Z. Hydrogen-bond-mediated *in situ* fabrication of AgNPs/Agar/PAN electrospun nanofibers as reproducible SERS substrates. *ACS Appl. Mater. Interfaces* **2015**, *7*, 1586–1594.

[136] Szymborski, T.; Witkowska, E.; Adamkiewicz, W.; Waluk, J.; Kamińska, A. Electrospun polymer mat as a SERS platform for the immobilization and detection of bacteria from fluids. *Analyst* **2014**, *139*, 5061–5064.

[137] Gong, Z. J.; Du, H. J.; Cheng, F. S.; Wang, C.; Wang, C. C.; Fan, M. K. Fabrication of SERS swab for direct detection of trace explosives in fingerprints. *ACS Appl. Mater. Interfaces* **2014**, *6*, 21931–21937.

[138] Qu, L.-L.; Geng, Y.-Y.; Bao, Z.-N.; Riaz, S.; Li, H. T. Silver nanoparticles on cotton swabs for improved surface-enhanced Raman scattering, and its application to the detection of carbaryl. *Microchim. Acta* **2016**, *183*, 1307–1313.

[139] Liu, Z. C.; Yan, Z. D.; Jia, L.; Song, P.; Mei, L. Y.; Bai, L.; Liu, Y. Q. Gold nanoparticle decorated electrospun nanofibers: A 3D reproducible and sensitive SERS substrate. *Appl. Surf. Sci.* **2017**, *403*, 29–34.

[140] Zhang, C.-L.; Lv, K.-P.; Huang, H.-T.; Cong, H.-P.; Yu, S.-H. Co-assembly of Au nanorods with Ag nanowires within polymer nanofiber matrix for enhanced SERS property by electrospinning. *Nanoscale* **2012**, *4*, 5348–5355.

[141] Tang, B.; Li, J. L.; Hou, X. L.; Afrin, T.; Sun, L.; Wang, X. G. Colorful and antibacterial silk fiber from anisotropic silver nanoparticles. *Ind. Eng. Chem. Res.* **2013**, *52*, 4556–4563.

[142] Camposeo, A.; Spadaro, D.; Magrì, D.; Moffa, M.; Gucciardi, P. G.; Persano, L.; Maragò, O. M.; Pisignano, D. Surface-enhanced Raman spectroscopy in 3D electrospun nanofiber mats coated with gold nanorods. *Anal. Bioanal. Chem.* **2016**, *408*, 1357–1364.

[143] Wang, L.; Sun, Y. J.; Wang, J. K.; Li, Z. Assembly of gold nanoparticles on electrospun polymer nanofiber film for SERS applications. *Bull. Korean Chem. Soc.* **2014**, *35*, 30–34.

[144] Zhang, W.-Y.; Xiao, X.-Z.; Lv, C.; Zhao, J.; Wang, G.; Gu, X.; Zhang, R.; Xu, B.-B.; Zhang, D.-D.; Li, A.-W. et al. Fabrication of photopolymer hierarchical micronanostructures by coupling electrospinning and photolithography for SERS substrates. *Macromol. Res.* **2013**, *21*, 306–310.

[145] Ren, S. X.; Dong, L. L.; Zhang, X. Q.; Lei, T. Z.; Ehrenhauser, F.; Song, K. L.; Li, M. C.; Sun, X. X.; Wu, Q. L. Electrospun nanofibers made of silver nanoparticles, cellulose nanocrystals, and polyacrylonitrile as substrates for surface-enhanced Raman scattering. *Materials* **2017**, *10*, 68.

[146] Rivero, P. J.; Urrutia, A.; Goicoechea, J.; Arregui, F. J. Nanomaterials for functional textiles and fibers. *Nanoscale Res. Lett.* **2015**, *10*, 501.

[147] Johnston, J. H.; Lucas, K. A. Nanogold synthesis in wool fibres: Novel colourants. *Gold Bull.* **2011**, *44*, 85–89.

[148] Kelly, F. M.; Johnston, J. H. Colored and functional silver nanoparticle−wool fiber composites. *ACS Appl. Mater. Interfaces* **2011**, *3*, 1083–1092.

[149] Tang, B.; Zhang, M. W.; Hou, X. L.; Li, J. L.; Sun, L.; Wang, X. G. Coloration of cotton fibers with anisotropic silver nanoparticles. *Ind. Eng. Chem. Res.* **2012**, *51*, 12807–12813.

[150] Tang, B.; Wang, J. F.; Xu, S. P.; Afrin, T.; Xu, W. Q.; Sun, L.; Wang, X. G. Application of anisotropic silver nanoparticles: Multifunctionalization of wool fabric. *J. Colloid Interface Sci.* **2011**, *356*, 513–518.

[151] Zheng, Y. D.; Xiao, M. D.; Jiang, S. X.; Ding, F.; Wang, J. F. Coating fabrics with gold nanorods for colouring, UV-protection, and antibacterial functions. *Nanoscale* **2013**, *5*, 788–795.

[152] Wang, R. H.; Wang, X. W.; Xin, J. H. Advanced visible-light-driven self-cleaning cotton by Au/TiO_2/SiO_2 photocatalysts. *ACS Appl. Mater. Interfaces* **2010**, *2*, 82–85.

[153] Wang, L. L.; Zhang, X. T.; Li, B.; Sun, P. P.; Yang, J. K.; Xu, H. Y.; Liu, Y. C. Superhydrophobic and ultraviolet-blocking cotton textiles. *ACS Appl. Mater. Interfaces* **2011**, *3*, 1277–1281.

[154] Tang, B.; Sun, L.; Kaur, J.; Yu, Y.; Wang, X. G. *In-situ* synthesis of gold nanoparticles for multifunctionalization of silk fabrics. *Dye. Pigment.* **2014**, *103*, 183–190.

[155] Robinson, A. M.; Zhao, L. L.; Shah Alam, M. Y.; Bhandari, P.; Harroun, S. G.; Dendukuri, D.; Blackburn, J.; Brosseau, C. L. The development of "fab-chips" as low-cost, sensitive surface-enhanced Raman spectroscopy (SERS) substrates for analytical applications. *Analyst* **2015**, *140*, 779–785.

[156] Liu, J.; Zhou, J.; Tang, B.; Zeng, T.; Li, Y. L.; Li, J. L.; Ye, Y.; Wang, X. G. Surface enhanced Raman scattering (SERS) fabrics for trace analysis. *Appl. Surf. Sci.* **2016**, *386*, 296–302.

[157] Tran, C. D. *In situ* identification of paper chromatogram spots by surface enhanced Raman scattering. *J. Chromatogr. A* **1984**, *292*, 432–438.

[158] Cabalín, L. M.; Laserna, J. J. Fast spatially resolved surface-enhanced Raman spectrometry on a silver coated filter paper using charge-coupled device detection. *Anal. Chim. Acta* **1995**, *310*, 337–345.

[159] Lee, C. H.; Tian, L. M.; Singamaneni, S. Paper-based SERS swab for rapid trace detection on real-world surfaces. *ACS Appl. Mater. Interfaces* **2010**, *2*, 3429–3435.

[160] Nergiz, S. Z.; Gandra, N.; Farrell, M. E.; Tian, L. M.; Pellegrino, P. M.; Singamaneni, S. Biomimetic SERS substrate: Peptide recognition elements for highly selective chemical detection in chemically complex media. *J. Mater. Chem. A* **2013**, *1*, 6543–6549.

[161] Webb, J. A.; Aufrecht, J.; Hungerford, C.; Bardhan, R. Ultrasensitive analyte detection with plasmonic paper dipsticks and swabs integrated with branched nanoantennas. *J. Mater. Chem. C* **2014**, *2*, 10446–10454.

[162] Diagnostic anSERS Inc. *Sensitive, flexible SERS substrates for your chemical diagnostic needs* [Online]. https://www.diagnosticansers.com/(accessed Oct 14, 2017).

[163] Tian, L. M.; Tadepalli, S.; Hyun Park, S.; Liu, K.-K.; Morrissey, J. J.; Kharasch, E. D.; Naik, R. R.; Singamaneni, S. Bioplasmonic calligraphy for multiplexed label-free biodetection. *Biosens. Bioelectron.* **2014**, *59*, 208–215.

[164] Tian, L. M.; Tadepalli, S.; Farrell, M. E.; Liu, K.-K.; Gandra, N.; Pellegrino, P. M.; Singamaneni, S. Multiplexed charge-selective surface enhanced Raman scattering based on plasmonic calligraphy. *J. Mater. Chem. C* **2014**, *2*, 5438–5446.

[165] Yu, W. W.; White, I. M. Inkjet-printed paper-based SERS dipsticks and swabs for trace chemical detection. *Analyst* **2013**, *138*, 1020–1025.

[166] Yu, W. W.; White, I. M. Chromatographic separation and detection of target analytes from complex samples using inkjet printed SERS substrates. *Analyst* **2013**, *138*, 3679–3686.

[167] Berger, A. G.; Restaino, S. M.; White, I. M. Vertical-flow paper SERS system for therapeutic drug monitoring of flucytosine in serum. *Anal. Chim. Acta* **2017**, *949*, 59–66.

[168] Berger, A. G.; White, I. M. Therapeutic drug monitoring of flucytosine in serum using a SERS-active membrane system. In *Proc. SPIE 10081, Frontiers in Biological Detection: From Nanosensors to Systems IX*, San Francisco, California, USA, **2017**; pp. 1008104.

[169] Maneeprakorn, W.; Bamrungsap, S.; Apiwat, C.; Wiriyachaiporn, N. Surface-enhanced Raman scattering based lateral flow immunochromatographic assay for sensitive influenza detection. *RSC Adv.* **2016**, *6*, 112079–112085.

[170] Abbas, A.; Brimer, A.; Slocik, J. M.; Tian, L. M.; Naik, R. R.; Singamaneni, S. Multifunctional analytical platform on a paper strip: Separation, preconcentration, and subattomolar detection. *Anal. Chem.* **2013**, *85*, 3977–3983.

[171] Yu, W. W.; White, I. M. A simple filter-based approach to surface enhanced Raman spectroscopy for trace chemical detection. *Analyst* **2012**, *137*, 1168–1173.

[172] Shi, Y.-E.; Li, L. M.; Yang, M.; Jiang, X. H.; Zhao, Q. Q.; Zhan, J. H. A disordered silver nanowires membrane for extraction and surface-enhanced Raman spectroscopy detection. *Analyst* **2014**, *139*, 2525–2530.

[173] Prikhozhdenko, E. S.; Lengert, E. V.; Parakhonskiy, B. V.; Gorin, D. A.; Sukhorukov, G. B.; Yashchenok, A. M. Biocompatible chitosan nanofibers functionalized with silver nanoparticles for SERS based detection. *Acta Phys. Pol. A* **2016**, *129*, 247–249.

[174] Prikhozhdenko, E. S.; Atkin, V. S.; Parakhonskiy, B. V.; Rybkin, I. A.; Lapanje, A.; Sukhorukov, G. B.; Gorin, D. A.; Yashchenok, A. M. New post-processing method of preparing nanofibrous SERS substrates with a high density of silver nanoparticles. *RSC Adv.* **2016**, *6*, 84505–84511.

[175] Gao, W. R.; Chen, G.; Xu, W. Q.; Yang, C. G.; Xu, S. P. Surface-enhanced Raman scattering (SERS) chips made from metal nanoparticle-doped polymer fibers. *RSC Adv.* **2014**, *4*, 23838–23845.

[176] Shao, J. D.; Tong, L. P.; Tang, S. Y.; Guo, Z. N.; Zhang, H.; Li, P. H.; Wang, H. Y.; Du, C.; Yu, X. F. PLLA nanofibrous paper-based plasmonic substrate with tailored hydrophilicity for focusing SERS detection. *ACS Appl. Mater. Interfaces* **2015**, *7*, 5391–5399.

[177] Jalaja, K.; Bhuvaneswari, S.; Ganiga, M.; Divyamol, R.; Anup, S.; Cyriac, J.; George, B. K. Effective SERS detection using a flexible wiping substrate based on electrospun polystyrene nanofibers. *Anal. Methods* **2017**, *9*, 3998–4003.